

# Statistical process control via $p$ -values

Hien Duy Nguyen<sup>1,2</sup> and Dan Wang<sup>2,3</sup>

January 27, 2026

<sup>1</sup>Institute of Mathematics for Industry, Kyushu University, Japan. <sup>2</sup>School of Computing, Engineering, and Mathematical Sciences, La Trobe University, Australia. <sup>3</sup>Department of Statistics, School of Mathematics, Northwest University, Xi'an, China

## Abstract

We study statistical process control (SPC) through charting of  $p$ -values. When in control (IC), any valid sequence  $(P_t)_t$  is super-uniform, a requirement that can hold in nonparametric and two-phase designs without parametric modelling of the monitored process. Within this framework, we analyse the Shewhart rule that signals when  $P_t \leq \alpha$ . Under super-uniformity alone, and with no assumptions on temporal dependence, we derive universal IC lower bounds for the average run length (ARL) and for the expected time to the  $k$ th false alarm ( $k$ -ARL). When conditional super-uniformity holds, these bounds sharpen to the familiar  $\alpha^{-1}$  and  $k\alpha^{-1}$  rates, giving simple, distribution-free calibration for  $p$ -value charts. Beyond thresholding, we use merging functions for dependent  $p$ -values to build EWMA-like schemes that output, at each time  $t$ , a valid  $p$ -value for the hypothesis that the process has remained IC up to  $t$ , enabling smoothing without ad hoc control limits. We also study uniform EWMA processes, giving explicit distribution formulas and left-tail guarantees. Finally, we propose a modular approach to directional and coordinate localisation in multivariate SPC via closed testing, controlling the family-wise error rate at the time of alarm. Numerical examples illustrate the utility and variety of our approach.

**Keywords:** statistical process control;  $p$ -values; exponentially weighted moving average; average run length; directional localisation

## 1 Introduction

Statistical process control (SPC) comprises an important class of methods for monitoring the behaviour of manufacturing, engineering, and other production processes. Since their introduction by Shewhart (1931), the SPC literature has grown significantly, with works such as Zwetsloot &

Woodall (2021), Waqas et al. (2024), Ahmed et al. (2025), and Tsung et al. (2025) providing good recent references on the current state of the art. Good introductions to the SPC literature appear in the texts of Xie et al. (2002), Qiu (2013), and Chakraborti & Graham (2019).

Typically, when conducting SPC, one seeks to monitor a process whose in-control state can be characterised as generating data from a null distribution, defined by a null hypothesis  $H_0$ . One then wishes to detect whether the process becomes out-of-control (OOC), characterised as a deviation away from  $H_0$ . In the discrete-time setting, at time point  $t \in \mathbb{N}$ , the analyst assesses deviation from the in-control (IC) state by sampling  $n_t \in \mathbb{N}$  observations from the data-generating process (DGP) and computing a test statistic  $Z_t$  whose distributional characteristics are known under  $H_0$ . The analyst then monitors the sequence of test statistics  $(Z_t)_t$  and raises an alarm whenever the test of  $H_0$  using  $Z_t$  is rejected at some specified level  $\alpha > 0$ . This choice controls the instantaneous false-alarm rate (FAR) of the monitoring process and the IC average run length, typically via a control limit for  $Z_t$  that can be characterised as a hypothesis-testing critical value depending on  $\alpha$ . This is the essence of the general scheme introduced by Shewhart (1931). A more sophisticated analyst can further employ time-point averaging methods, such as the cumulative sum (CUSUM) and exponentially weighted moving average (EWMA) charts introduced by Page (1954) and Roberts (1959), respectively. The null distributions of these chart statistics can be obtained in specific parametric situations, such as under assumptions of normality (see, e.g., Roberts, 1959, Lucas & Saccucci, 1990, Lowry et al., 1992, Lu & Reynolds, 1999, Yeh et al., 2003, and Knoth, 2005), but can be difficult to deduce in general.

For any hypothesis  $H_0$ , one can typically construct a sequence of  $p$ -values  $(P_t)_t$ , based on samples of sizes  $(n_t)_t$ , which can be used as test statistics for  $H_0$  in place of  $(Z_t)_t$ . Here, we define the  $p$ -value as a random variable  $P$  taking values in the unit interval such that, under the null  $H_0$ , the probability that  $P \leq \alpha$  is less than or equal to  $\alpha$  for each  $\alpha > 0$ , following the general definition of Lehmann & Romano (2022). The use of  $p$ -values in SPC has been explored in the works of Grigg & Spiegelhalter (2008), who derive and make use of the steady-state distribution of CUSUM statistics to compute  $p$ -values for monitoring; Grigg et al. (2009) and Li & Tsung (2009), who consider the use of  $p$ -values and false discovery rate control to simultaneously monitor multiple processes; and Li et al. (2013), who suggest the charting of  $p$ -values as a unified framework for conducting SPC, particularly in the presence of variable sampling intervals (VSI) and variable sample sizes (VSS) in each time period.

In this work, we continue to develop the use of the  $p$ -value as a charting tool for SPC. In particular, we demonstrate that  $p$ -values are applicable in both one- and two-phase monitoring programmes and, like Li et al. (2013), we discuss how  $p$ -values are applicable in VSI and VSS settings. Without any assumption on stochastic dependence within the sequence  $(P_t)_t$ , we prove that the  $p$ -value chart that raises an alarm if  $P_t \leq \alpha$  has an average run length (ARL) that is always bounded below by  $(1 + \alpha^{-1})/2$ , and under a conditional super-uniformity assumption, we prove that this can be improved to the typical  $\alpha^{-1}$  bound of parametric methods. To extend these

observations, motivated by the notion of  $k$ -FWER (generalised family-wise error rate; the case  $k = 1$  corresponds to the usual family-wise error rate (FWER); Lehmann & Romano, 2005), we also study the  $k$ -ARL, defined as the average time until first observing  $k$  false alarms under the null hypothesis, which generalises the usual ARL (corresponding to the  $k = 1$  case). Without dependence assumptions, we prove that  $k$ -ARL is bounded below by  $(1 + k\alpha^{-1})/2$ , which again improves to  $k\alpha^{-1}$  under conditional super-uniformity assumptions. These  $k$ -ARL bounds allow the  $p$ -value charts to be correctly calibrated for all DGPs where  $H_0$  holds and mitigate against the time-consuming task of simulation-based ARL calibration, which only holds under the specific DGP assumptions that underlie the simulation study.

Further to these results, we demonstrate that, like well-behaved test statistics, one can construct EWMA-like schemes  $(Q_t)_t$  based on a  $p$ -value sequence  $(P_t)_t$ , such that each  $Q_t$  is a  $p$ -value for the hypothesis that  $H_0$  is true for all time points up to time  $t$ , against the complementary hypothesis. We demonstrate that this is possible using recent results for combining  $p$ -values (Vovk & Wang, 2020; Vovk et al., 2022). Thus, given any sequence of test statistics  $(Z_t)_t$  whose null distributions admit  $p$ -values, one can always generate EWMA-like schemes for SPC. We further consider and follow on from the work on EWMA charts based on uniform test-statistic constructions of Yeh et al. (2003) and obtain novel results regarding the weighted averaging of independent and identically distributed random variables. This permits the general and generic construction of EWMA versions of one-phase parametric Shewhart-type charts with ARL control that does not depend on simulated calibration or specific test statistic distributions.

Using a  $p$ -value-based closed-testing procedure (e.g., Marcus et al., 1976), we show how  $p$ -value charts can detect any departure of the multivariate parameter from a null baseline as well as localise the affected coordinates and directions of deviation, in a principled way, with simultaneous error control. This provides an alternative to the test-statistic-based approaches to the same problem of Hawkins (1991), Mason et al. (1995), Tan & Shi (2012), Xu et al. (2023), Xu & Deng (2023), and Xiong & Xu (2025), for example. We then conclude with demonstrations of the validity and applicability of our approaches via examples and numerical simulations, where we present novel methods for monitoring the stability of the distribution of a process using  $p$ -values from Kolmogorov–Smirnov tests, and provide a nonparametric method for localising the direction and coordinate of change via Mann–Whitney  $U$ -tests (see Gibbons & Chakraborti, 2010 regarding nonparametric tests).

The remainder of the manuscript proceeds as follows. In Section 2, we present our general technical framework, together with our ARL results and EWMA constructions. Section 3 then contains the application of  $p$ -values to the problem of localised detection for multivariate charts. Examples and numerical simulations are presented in Section 4, and Section 5 contains concluding remarks. Proofs of theorems and additional technical and numerical results appear in the Appendix.

## 2 Main results

### 2.1 Technical setup

Let  $(\Omega, \mathfrak{A}, P)$  be a probability space on which all of our random objects are supported, with generic element  $\omega$  and expectation symbol  $E$ . We suppose that the fundamental object that we wish to monitor via an SPC process is the random object  $X : \Omega \rightarrow \mathbb{X}$ , where  $(\mathbb{X}, \mathfrak{B}_{\mathbb{X}})$  is a metric space equipped with its Borel  $\sigma$ -algebra. For each  $t \in \mathbb{N}$ , let  $X_t$  denote a time- $t$  replicate of  $X$  and let  $P_{X,t} \in \mathcal{M}_{\mathbb{X}}$  denote the push-forward measure of  $X_t$  at time  $t$ , where  $\mathcal{M}_{\mathbb{X}}$  is the set of Borel probability measures on  $\mathbb{X}$ . We will say that the process is IC at time  $t$  if  $P_{X,t}$  satisfies the null hypothesis  $H_0$ , where the null hypothesis is some property of a measure in  $\mathcal{M}_{\mathbb{X}}$  (e.g., if  $\mathbb{X} = \mathbb{R}$ ,  $H_0$  may be that  $EX_t = 0$ ).

We consider two types of SPC designs: the one-phase and the two-phase designs. In the one-phase design, at each time  $t$ , we realise an IID sample  $\mathbf{X}_t = (X_{t,i})_i$  of replicates of  $X_t$  with probability measure  $P_{X,t}$ , for  $i \in [n_t] = [1, n_t] \cap \mathbb{N}$ . Using  $(\mathbf{X}_t)_t$ , we then compute the  $p$ -value  $P_t = p_t(\mathbf{X}_1, \dots, \mathbf{X}_t)$  for some functions  $p_t : \mathbb{X}^{\sum_{s=1}^t n_s} \rightarrow [0, 1]$ , and say that  $(P_t)_t$  satisfies the super-uniformity property (under  $H_0$ ) if, for each  $t$ ,

$$P_{0,t}(P_t \leq \alpha) \leq \alpha, \text{ for every } \alpha \in [0, 1] \text{ and every } P_{0,t} \in \mathcal{M}_{0,t}. \quad (1)$$

Here,  $\mathcal{M}_{0,t}$  denotes the set of probability measures  $P_{0,t}$  on  $(\Omega, \mathfrak{A})$  such that the push-forward measure of  $X_s$  under  $P_{0,t}$  satisfies  $H_0$ , for every  $s \in [t]$ .

Alternatively, in a two-phase design we first realise a so-called Phase I sample  $\mathbf{X}_0 = (X_{0,i})_i$  of IID replicates of  $X_0$  with measure  $P_{X,0}$ , where  $i \in [n_0]$ . The null hypothesis  $H_0$  is then defined relative to the measure  $P_{X,0}$ ; for example, we may consider the equality in distribution hypothesis that  $P_{X,t} = P_{X,0}$ . Like the one-phase design, we then realise IID samples  $(X_{t,i})_i$  at each time  $t$  of size  $n_t$ , arising from the measure  $P_{X,t}$ . Since  $H_0$  at each  $t$  is a hypothesis concerning  $P_{X,0}$  along with the measures  $P_{X,t}$ , the  $p$ -value for the test must be taken as a function of both samples  $\mathbf{X}_0$  and  $\mathbf{X}_1, \dots, \mathbf{X}_t$ :  $P_t = p_t(\mathbf{X}_0, \dots, \mathbf{X}_t)$  for some  $p_t : \mathbb{X}^{\sum_{s=0}^t n_s} \rightarrow [0, 1]$ , and again is taken to satisfy the super-uniformity property (1).

In either case, we obtain a sequence of  $p$ -values  $(P_t)_t$  that test  $H_0$  at each time point  $t$ , where we do not assume any particular temporal dependence structure between the  $p$ -values. The sequence constitutes a control chart and an alarm is triggered at time  $t$  if  $P_t < \alpha$  for some control limit  $\alpha$  chosen by the analyst. Here, the control limit is the usual size of the hypothesis test for  $H_0$ , and the super-uniformity property ensures that, under  $H_0$ , the probability of a false alarm at time  $t$  is at most  $\alpha$ .

## 2.2 Controlling the average run length

The ARL is defined as the expected time to first alarm, assuming that  $P_{X,t}$  satisfies  $H_0$  for each time  $t$ . Let  $R : \Omega \rightarrow \mathbb{N}$  denote the run length. For each  $m \in \mathbb{N}$ , we can write

$$P_0(R \leq m) = P_0 \left( \bigcup_{t=1}^m \{P_t \leq \alpha\} \right) \leq \sum_{t=1}^m P_0(P_t \leq \alpha) \leq m\alpha,$$

by super-uniformity, where  $P_0$  is any measure on  $(\Omega, \mathfrak{A})$  in  $\mathcal{M}_{0,t}$  for all  $t \in \mathbb{N}$ . We thus have  $P_0(R > m) \geq 1 - m\alpha$  for every  $m \geq 0$ , and thus for each  $m \geq 1$ ,

$$P_0(R \geq m) = P_0(R > m - 1) \geq 1 - (m - 1)\alpha.$$

Using the survival function expression for the expectation (cf. Gut, 2013, Thm. 12.1, p. 75), we can express the ARL as

$$\text{ARL} = E_0 R = \sum_{m=1}^{\infty} P_0(R \geq m) \geq \sum_{m=1}^{\infty} [1 - (m - 1)\alpha]_+, \quad (2)$$

where  $E_0$  is the expectation operator for  $P_0$  and  $[a]_+ = \max\{a, 0\}$ .

**Proposition 1.** *For each  $\alpha \in (0, 1]$ , if  $(P_t)_t$  satisfies (1), then*

$$\text{ARL} \geq \frac{1}{2\alpha} + \frac{1}{2}.$$

*Proof.* All proofs appear in the Appendix.  $\square$

The bound above can be improved given some assumptions on conditional super-uniformity of the  $p$ -values. In particular, suppose that  $(\mathcal{F}_t)_t$  is a filtration on the space  $(\Omega, \mathfrak{A})$ , whereupon the following assumption holds:

$$P_0(P_t \leq \alpha \mid \mathcal{F}_{t-1}) \leq \alpha, \text{ a.s., for every } \alpha \in [0, 1]. \quad (3)$$

**Proposition 2.** *Suppose that  $(P_t)_t$  satisfies (3) for some filtration  $(\mathcal{F}_t)_t$ . Then, for each  $\alpha \in (0, 1]$ ,*

$$\text{ARL} \geq \frac{1}{\alpha}.$$

With  $\mathcal{F}_t = \sigma(\mathbf{X}_1, \dots, \mathbf{X}_t)$ , observe that the conditional super-uniformity assumption (3) is satisfied in the one-phase design whenever the  $p$ -value at time  $t$  depends only on the time- $t$  sample  $\mathbf{X}_t$  and  $\mathbf{X}_t$  is independent of  $\mathcal{F}_{t-1}$  under  $P_0$ , i.e.,  $P_t = p_t(\mathbf{X}_t)$ . Similarly, for a two-phase design, with  $\mathcal{F}_t = \sigma(\mathbf{X}_0, \mathbf{X}_1, \dots, \mathbf{X}_t)$ , the condition is satisfied whenever the time- $t$   $p$ -value depends only on the Phase I sample  $\mathbf{X}_0$  and the time- $t$  sample  $\mathbf{X}_t$  and  $\mathbf{X}_t$  is conditionally independent of

$(\mathbf{X}_1, \dots, \mathbf{X}_{t-1})$  given  $\mathbf{X}_0$  under  $P_0$ , i.e.,  $P_t = p_t(\mathbf{X}_0; \mathbf{X}_t)$ . These are among the most common cases for  $p$ -value constructions, and thus the assumption can be considered reasonable. In the sequel, we will show that certain EWMA-like schemes also satisfy condition (3).

We note that the bound of Proposition 2 is, in fact, tight. This can be seen by considering an IID sequence  $(P_t)_t$  adapted to  $(\mathcal{F}_t)_t$ , where  $P_t \sim \text{Unif}(0, 1)$  under  $H_0$  and therefore  $P_0(P_t \leq \alpha \mid \mathcal{F}_{t-1}) = \alpha$  for each  $\alpha \in [0, 1]$  and  $t \in \mathbb{N}$ , thus satisfying (3). It then holds that  $P_0(R > t) = (1 - \alpha)^t$  and therefore  $E_0 R = \alpha^{-1}$ . This is the usual computation of the ARL for parametric Shewhart-type charts (see, e.g., Chakraborti & Graham, 2019, Sec. 3.6.1).

### 2.3 Controlling the $k$ -ARL

Like the ARL, we define the  $k$ -ARL as the expected time until  $k$  alarms are raised, assuming that  $P_{X,t}$  satisfies  $H_0$  for each time  $t$ , and let  $R_k : \Omega \rightarrow \mathbb{N}$  denote the time until  $k$  alarms are raised. That is, the  $k$ -ARL is equal to  $E_0 R_k$ . Note that the usual ARL and run length are the 1-ARL and  $R_1$ , respectively. Under only super-uniformity, we have the following result.

**Proposition 3.** *For each  $\alpha \in (0, 1]$ , if  $(P_t)_t$  satisfies (1), then, for any  $k \geq 1$ ,*

$$E_0 R_k \geq (\nu + 1) \left(1 - \frac{\alpha\nu}{2k}\right) \geq \frac{k}{2\alpha} + \frac{1}{2},$$

where  $\nu = \lfloor k/\alpha \rfloor$ .

Under the stronger assumption of Proposition 2, we also have an analogous result for controlling the  $k$ -ARL. Unfortunately, we do not know an elementary proof of this result, as we did for Proposition 2, and must instead resort to martingale theory.

**Proposition 4.** *Suppose that  $(P_t)_t$  satisfies (3) for some filtration  $(\mathcal{F}_t)_t$ . Then, for each  $\alpha \in (0, 1]$  and  $k \geq 1$ ,*

$$E_0 R_k \geq \frac{k}{\alpha}.$$

We note that we are not the first to study the time to  $k$  alarms,  $R_k$ , although we cannot find specific instances of the  $k$ -ARL being studied in the  $p$ -value context in the literature. Prior work includes the study of  $k > 1$  failure rules for negative binomial charts (Albers, 2010, 2011), and conforming-count charts (CCC- $r$ ) (Xie et al., 1998; Ohta et al., 2001; Joeckes et al., 2016; Chen, 2025). In these works, the control of the  $k$ -ARL is considered parametrically under a negative binomial model, in which conformity of the process being measured is treated as an IID Bernoulli event. In contrast, our approach is model-free and relies only on the availability of super-uniform  $p$ -values that satisfy either (1) or (3).

Finally, we note that the bound from Proposition 4 is sharp by the same reasoning as that of Proposition 2. Namely, suppose that we take  $P_t \sim \text{Unif}(0, 1)$  IID and independent of  $\mathcal{F}_{t-1}$ .

Let  $I_t$  denote the indicator of the event  $\{P_t \leq \alpha\}$ . Then,  $(I_t)_t$  are IID  $\text{Bern}(\alpha)$ . If we define  $G_1 = \inf\{t \geq 1 : I_t = 1\}$  and  $G_j = \inf\{t \geq 1 : \sum_{s=1}^t I_s = j\} - \inf\{t \geq 1 : \sum_{s=1}^t I_s = j-1\}$ , for each  $j \geq 2$ , then  $G_j \sim \text{Geom}(\alpha)$  for each  $j \in \mathbb{N}$ , where  $G_j$  is the inter-alarm waiting time and  $E_0 G_j = 1/\alpha$ . Then, the time to  $k$  alarms is simply the sum of the first  $k$  inter-alarm times:  $R_k = \sum_{j=1}^k G_j$ , and by linearity, we have  $E_0 R_k = k/\alpha$ .

## 2.4 Exponentially weighted moving average charts

To construct our exponentially weighted moving average charts, we rely on results from Vovk & Wang (2020) that permit us to average arbitrarily dependent  $p$ -values. For  $p$ -values  $P_1, \dots, P_m$  satisfying (1), weights  $\mathbf{w} = (w_1, \dots, w_m) \in [0, 1]^m$  such that  $\sum_{t=1}^m w_t = 1$ , and  $r > -1$  with  $r \neq 0$ , we define the weighted generalised mean

$$(p_1, \dots, p_m) \mapsto M_{r, \mathbf{w}}(p_1, \dots, p_m) = \left( \sum_{t=1}^m w_t p_t^r \right)^{1/r}.$$

We say that the function  $q : [0, 1]^m \rightarrow \mathbb{R}_{\geq 0}$  is a valid merging function if  $P_0(q(P_1, \dots, P_m) \leq \alpha) \leq \alpha$  for each  $\alpha \in [0, 1]$ . The following result is a consequence of Vovk & Wang (2020).

**Lemma 5.** *Let  $r > -1$  with  $r \neq 0$  and  $w_{\max} = \max_{t \in [m]} w_t$ .*

1. *For  $r > -1$ , the map*

$$q = (1 + r)^{1/r} M_{r, \mathbf{w}}$$

*is a valid merging function.*

2. *For  $r \in [1, \infty)$ , the map*

$$q = (\min\{1 + r, w_{\max}^{-1}\})^{1/r} M_{r, \mathbf{w}}$$

*is a valid merging function.*

For a generic sequence of test statistics  $(Z_t)_t$  and a learning rate  $\lambda \in (0, 1)$ , an EWMA chart  $(\tilde{Z}_{\lambda, t})_t$  is typically defined via the one-step expression:

$$\tilde{Z}_{\lambda, t} = \lambda Z_t + (1 - \lambda) \tilde{Z}_{\lambda, t-1},$$

for each  $t \in \mathbb{N}$ , given some initial  $\tilde{Z}_{\lambda, 0}$ . Unfortunately, such a scheme is not implementable for  $p$ -values, in the sense that if  $(P_t)_t$  satisfies (1) and

$$\tilde{P}_{\lambda, t} = \lambda P_t + (1 - \lambda) \tilde{P}_{\lambda, t-1},$$

then  $(\tilde{P}_{\lambda, t})_t$  need not be a sequence of super-uniform  $p$ -values under  $P_0$ . We thus require a modified approach, making use of Lemma 5.

### 2.4.1 EWMA-like charts via $p$ -value averaging

Starting with  $(P_t)_{t \in \mathbb{N}}$  satisfying (1), for each  $\lambda \in (0, 1)$  and  $r > -1$  with  $r \neq 0$  we define the EWMA recursion directly from the first  $p$ -value by

$$S_{\lambda,1}^{(r)} = P_1^r, \text{ and } S_{\lambda,t}^{(r)} = \lambda P_t^r + (1 - \lambda) S_{\lambda,t-1}^{(r)}, \text{ for } t \geq 2.$$

By induction one checks that, for each  $t \in \mathbb{N}$ ,

$$S_{\lambda,t}^{(r)} = \sum_{s=1}^t w_{t,s} P_s^r, \quad w_{t,1} = (1 - \lambda)^{t-1}, \text{ and } w_{t,s} = \lambda(1 - \lambda)^{t-s}, \text{ for } 2 \leq s \leq t, \quad (4)$$

so that  $w_{t,s} \geq 0$  and  $\sum_{s=1}^t w_{t,s} = 1$ .

Let

$$w_{t,\max} = \max_{1 \leq s \leq t} w_{t,s} = \max \{ \lambda, (1 - \lambda)^{t-1} \}.$$

For each  $\lambda \in (0, 1)$ ,  $r > -1$  with  $r \neq 0$ , and  $t \in \mathbb{N}$  we now set

$$a_{\lambda,t}^{(r)} = \begin{cases} \min \left\{ 1 + r, \frac{1}{w_{t,\max}} \right\}^{1/r} & \text{if } r \geq 1, \\ (1 + r)^{1/r} & \text{if } r \in (-1, 1) \setminus \{0\}, \end{cases} \quad \text{and } Q_{\lambda,t}^{(r)} = a_{\lambda,t}^{(r)} \left[ S_{\lambda,t}^{(r)} \right]^{1/r}. \quad (5)$$

The fact that  $\left( Q_{\lambda,t}^{(r)} \right)_t$  is EWMA-like can be seen most clearly when  $r = 1$ , in which case

$$Q_{\lambda,1}^{(1)} = P_1$$

and, for each  $t \geq 2$ ,

$$Q_{\lambda,t}^{(1)} = a_{\lambda,t}^{(1)} \left\{ \lambda P_t + (1 - \lambda) \frac{Q_{\lambda,t-1}^{(1)}}{a_{\lambda,t-1}^{(1)}} \right\}, \quad (6)$$

so that  $Q_{\lambda,t}^{(1)}$  is a rescaled EWMA of the  $p$ -values  $P_t$ .

**Proposition 6.** *For each  $\lambda \in (0, 1)$  and  $r > -1$  with  $r \neq 0$ , if  $(P_t)_t$  satisfies (1), then the sequence  $\left( Q_{\lambda,t}^{(r)} \right)_{t \in \mathbb{N}}$  defined in (4)–(5) is super-uniform under  $P_0$ , i.e. for each  $\alpha \in [0, 1]$ ,*

$$P_0 \left( Q_{\lambda,t}^{(r)} \leq \alpha \right) \leq \alpha \quad \text{for all } t \in \mathbb{N}.$$

A notable inconvenience in applying Proposition 6 when  $r \geq 1$  is that the constants  $\left( a_{\lambda,t}^{(r)} \right)_t$  are not time-independent. At some loss of sharpness in the super-uniform inequality, we can replace  $a_{\lambda,t}^{(r)}$  by a time-independent bound  $a_{\lambda}^{(r)}$  that works for all  $t$ . Since  $w_{t,\max} \geq \lambda$  for every  $t \geq 1$ , we

have  $w_{t,\max}^{-1} \leq \lambda^{-1}$  and therefore

$$\min\{1+r, w_{t,\max}^{-1}\} \leq \min\{1+r, \lambda^{-1}\}.$$

Define

$$a_\lambda^{(r)} = \begin{cases} \min\{1+r, \frac{1}{\lambda}\}^{1/r} & \text{if } r \geq 1, \\ (1+r)^{1/r} & \text{if } r \in (-1, 1) \setminus \{0\}, \end{cases} \quad \text{and } \tilde{Q}_{\lambda,t}^{(r)} = a_\lambda^{(r)} [S_{\lambda,t}^{(r)}]^{1/r}. \quad (7)$$

Then  $a_\lambda^{(r)} \geq a_{\lambda,t}^{(r)}$  for every  $t$ , so

$$\tilde{Q}_{\lambda,t}^{(r)} = \frac{a_\lambda^{(r)}}{a_{\lambda,t}^{(r)}} Q_{\lambda,t}^{(r)} \geq Q_{\lambda,t}^{(r)}.$$

Hence  $\{\tilde{Q}_{\lambda,t}^{(r)} \leq \alpha\} \subseteq \{Q_{\lambda,t}^{(r)} \leq \alpha\}$  for all  $\alpha \in [0, 1]$ , and the super-uniformity of  $Q_{\lambda,t}^{(r)}$  yields

$$P_0(\tilde{Q}_{\lambda,t}^{(r)} \leq \alpha) \leq P_0(Q_{\lambda,t}^{(r)} \leq \alpha) \leq \alpha, \quad \text{for all } t \in \mathbb{N}.$$

Another unfortunate inconvenience is that the EWMA-like  $p$ -values  $(Q_{\lambda,t}^{(r)})_t$  and their modification  $(\tilde{Q}_{\lambda,t}^{(r)})_t$  need not maintain *conditional* super-uniformity when the original sequence  $(P_t)_t$  satisfies the conditional super-uniformity condition (3). Fortunately, conditional super-uniformity is preserved for the modification

$$\bar{Q}_{\lambda,t}^{(r)} = \lambda^{-1/r} [S_{\lambda,t}^{(r)}]^{1/r}, \quad t \geq 1, \quad (8)$$

for each  $\lambda \in (0, 1)$ , when  $r \geq 1$ . In the special case  $r = 1$  we have

$$\bar{Q}_{\lambda,1}^{(1)} = \lambda^{-1} P_1 \quad \text{and} \quad \bar{Q}_{\lambda,t}^{(1)} = P_t + (1 - \lambda) \bar{Q}_{\lambda,t-1}^{(1)}, \quad t \geq 2,$$

so that  $\lambda \bar{Q}_{\lambda,t}^{(1)}$  is the usual EWMA of the raw  $p$ -values  $P_t$  with weight  $\lambda$  on the current observation.

**Proposition 7.** *For each  $\lambda \in (0, 1)$  and  $r \geq 1$ , suppose  $(P_t)_t$  satisfies (3) for the filtration  $(\mathcal{F}_t)_t$ . Define  $S_{\lambda,t}^{(r)}$  as above and  $\bar{Q}_{\lambda,t}^{(r)}$  by (8). Then  $(\bar{Q}_{\lambda,t}^{(r)})_t$  is conditionally super-uniform under  $P_0$ , i.e., for each  $\alpha \in [0, 1]$ ,*

$$P_0(\bar{Q}_{\lambda,t}^{(r)} \leq \alpha \mid \mathcal{F}_{t-1}) \leq \alpha, \quad \text{a.s., for all } t \geq 1.$$

*Remark 8.* For  $r \geq 1$ , when  $\lambda \geq 1/2$ , it holds that  $1/\lambda \leq 2 \leq 1+r$ , so  $a_\lambda^{(r)} = \lambda^{-1/r}$  and therefore  $\tilde{Q}_{\lambda,t}^{(r)} = \bar{Q}_{\lambda,t}^{(r)}$  for all  $t \geq 1$ . Moreover, for  $t \geq 2$  we have  $(1 - \lambda)^{t-1} \leq 1 - \lambda \leq \lambda$ , so  $w_{t,\max} = \lambda$ , hence  $a_{\lambda,t}^{(r)} = \lambda^{-1/r}$  and

$$Q_{\lambda,t}^{(r)} = \tilde{Q}_{\lambda,t}^{(r)} = \bar{Q}_{\lambda,t}^{(r)}, \quad \text{for } t \geq 2.$$

At time  $t = 1$  we have  $w_{1,\max} = 1$ , so  $a_{\lambda,1}^{(r)} = 1$  and  $Q_{\lambda,1}^{(r)} = P_1$  while  $\tilde{Q}_{\lambda,1}^{(r)} = \bar{Q}_{\lambda,1}^{(r)} = \lambda^{-1/r} P_1$ . Thus, for  $\lambda \geq 1/2$ , the only discrepancy between  $Q_{\lambda,t}^{(r)}$  and the conditionally valid  $\bar{Q}_{\lambda,t}^{(r)}$  occurs at the very

first time point.

When  $\lambda < 1/2$ , the quantities  $Q_{\lambda,t}^{(r)}$  and  $\tilde{Q}_{\lambda,t}^{(r)}$  can differ for early time points, because the maximal EWMA weight  $w_{t,\max} = \max\{\lambda, (1-\lambda)^{t-1}\}$  may be larger than  $\lambda$ . However, since  $(1-\lambda)^{t-1}$  decays geometrically in  $t$ , there exists a finite index  $t_{\max}(\lambda, r)$  such that  $Q_{\lambda,t}^{(r)} = \tilde{Q}_{\lambda,t}^{(r)}$  for all  $t > t_{\max}(\lambda, r)$ . Thus, for large  $t$  and  $\lambda < 1/2$  it suffices to work with the simpler, time-homogeneous EWMA-like chart  $(\tilde{Q}_{\lambda,t}^{(r)})_t$ .

An alternative construction of EWMA-like charts for  $p$ -value statistics is via the method of  $e$ -values. We provide such a derivation in the Appendix for completeness but note that the constructed objects did not perform as well in comparison to the averaging method above in external numerical assessments.

#### 2.4.2 The distribution of the EWMA process for independent uniform random variables

We conclude this section with an extension of the exploration of the EWMA process for IID uniform random variables, considered by Yeh et al. (2003). In particular, Yeh et al. (2003) consider a sequence of IID test statistics  $(Z_t)_t$ , whose distribution under  $H_0$  is equal to that of  $Z$ . Using the probability integral transformation (i.e., the cumulative distribution function (CDF) of  $Z$ ,  $F_Z$ ), the authors generate the sequence  $(U_t)_t$ , where, for each  $t$ ,  $U_t = F_Z(Z_t)$  has distribution  $\text{Unif}(0, 1)$  under  $H_0$  (when  $F_Z$  is continuous). The authors then consider the transformation  $V_t = U_t - 1/2$ , and construct the corresponding EWMA process  $(\tilde{V}_{\lambda,t})_t$ , defined by

$$\tilde{V}_{\lambda,t} = \lambda V_t + (1 - \lambda) \tilde{V}_{\lambda,t-1},$$

for  $\lambda \in (0, 1)$  and  $t \geq 1$ , with  $\tilde{V}_{\lambda,0} = 0$ . They proceed to produce mean and variance formulas for the process and obtain ARL estimates for various control rules via Monte Carlo simulation.

We follow on from their work by considering IID sequences  $(U_t)_t$  with  $U_t \sim \text{Unif}(0, 1)$  (we may regard  $P_t = U_t$  as a  $p$ -value under  $H_0$ ), and construct the EWMA process  $(\tilde{U}_{\lambda,t})_t$ , defined by

$$\tilde{U}_{\lambda,t} = \lambda U_t + (1 - \lambda) \tilde{U}_{\lambda,t-1},$$

for  $\lambda \in (0, 1)$  and  $t \geq 1$ , with  $\tilde{U}_{\lambda,0} = u_0 \in [0, 1]$ . Since  $V_t = U_t - 1/2$  and the EWMA recursion is linear, the two EWMA processes are related by

$$\tilde{U}_{\lambda,t} = \tilde{V}_{\lambda,t} + \frac{1}{2} + (1 - \lambda)^t \left( u_0 - \frac{1}{2} \right), \text{ for } t \geq 1,$$

where  $\left(\tilde{V}_{\lambda,t}\right)_t$  denotes the EWMA of  $V_t$  with  $\tilde{V}_{\lambda,0} = 0$ . In particular, when  $u_0 = 1/2$ ,

$$\tilde{U}_{\lambda,t} = \tilde{V}_{\lambda,t} + \frac{1}{2}, \text{ for all } t \geq 1,$$

so  $\left(\tilde{U}_{\lambda,t}\right)_t$  is a mean-shift of  $\left(\tilde{V}_{\lambda,t}\right)_t$  and thus characterises the same underlying stochastic object, up to an additive constant. We now present an expression for the probability density function (PDF) of  $\tilde{U}_{\lambda,t}$ , for each  $t \geq 1$ .

**Proposition 9.** *Let  $a_{t,s} = \lambda(1-\lambda)^{t-s}$  and  $a_{\mathbb{S}} = \sum_{s \in \mathbb{S}} a_{t,s}$ , for each  $s \in [t]$  and  $\mathbb{S} \subseteq [t]$ . Then, for each  $u_0 \in [0, 1]$  and  $t \geq 1$ , the PDF and CDF of  $\tilde{U}_{\lambda,t}$  have the respective forms:*

$$u \mapsto f_{t,u_0}(u) = \frac{1}{(t-1)! \prod_{s=1}^t a_{t,s}} \sum_{\mathbb{S} \subseteq [t]} (-1)^{|\mathbb{S}|} [u - (1-\lambda)^t u_0 - a_{\mathbb{S}}]_+^{t-1},$$

$$u \mapsto F_{t,u_0}(u) = \frac{1}{t! \prod_{s=1}^t a_{t,s}} \sum_{\mathbb{S} \subseteq [t]} (-1)^{|\mathbb{S}|} [u - (1-\lambda)^t u_0 - a_{\mathbb{S}}]_+^t.$$

From the linearity of expectation applied to  $\tilde{U}_{\lambda,t}$ , and the fact that  $E_0 U_t = 1/2$  and  $\text{var}_0(U_t) = 1/12$  (where  $\text{var}_0$  is the variance under  $H_0$ ), we have

$$E_0 \tilde{U}_{\lambda,t} = (1-\lambda)^t u_0 + \sum_{s=1}^t a_{t,s} E_0 U_s = \frac{1}{2} + (1-\lambda)^t \left(u_0 - \frac{1}{2}\right),$$

and, by independence of  $(U_t)_t$ ,

$$\text{var}_0(\tilde{U}_{\lambda,t}) = \sum_{s=1}^t a_{t,s}^2 \text{var}_0(U_s) = \frac{1}{12} \frac{\lambda [1 - (1-\lambda)^{2t}]}{2 - \lambda}.$$

These expressions match those obtained by Yeh et al. (2003).

As we stated at the start of the section, the EWMA  $p$ -values  $\left(\tilde{P}_{\lambda,t}\right)_t$  need not be super-uniform under  $H_0$ , in general. We validate this claim by showing (i) if  $u_0 < 1$ , then  $\tilde{U}_{\lambda,t}$  is not super-uniform for every  $t \geq 1$  and  $\lambda \in (0, 1)$ ; and (ii) when  $u_0 = 1$ , the only globally super-uniform case is  $t = 1$ , whereas for  $t \geq 2$  super-uniformity fails.

For (i), note that since  $a_{t,s} U_s : \Omega \rightarrow [0, a_{t,s}]$  for each  $s$ ,

$$\sum_{s=1}^t a_{t,s} U_s : \Omega \rightarrow \left[0, \sum_{s=1}^t a_{t,s}\right] = \left[0, 1 - (1-\lambda)^t\right].$$

Because  $\tilde{U}_{\lambda,t} = (1-\lambda)^t u_0 + \sum_{s=1}^t a_{t,s} U_s$ ,

$$\tilde{U}_{\lambda,t} : \Omega \rightarrow \left[(1-\lambda)^t u_0, 1 - (1-\lambda)^t (1 - u_0)\right].$$

Hence, if  $\alpha^*$  satisfies  $1 - (1 - \lambda)^t(1 - u_0) < \alpha^* < 1$ , then  $P_0(\tilde{U}_{\lambda,t} \leq \alpha^*) = 1 > \alpha^*$ , so  $\tilde{U}_{\lambda,t}$  is not super-uniform with respect to  $P_0$ . In particular, if  $u_0 < 1$ , such an  $\alpha^*$  always exists.

For (ii), take  $u_0 = 1$ , so  $\text{supp}(\tilde{U}_{\lambda,t}) = [(1 - \lambda)^t, 1]$ . When  $t = 1$ ,  $\tilde{U}_{\lambda,1} \sim \text{Unif}(1 - \lambda, 1)$  and is globally super-uniform. For  $t \geq 2$ , define the normalised convex combination

$$\bar{U}_{\lambda,t} = \frac{\tilde{U}_{\lambda,t} - (1 - \lambda)^t}{1 - (1 - \lambda)^t} = \sum_{s=1}^t w_s U_s, \quad w_s = \frac{a_{t,s}}{1 - (1 - \lambda)^t}, \quad \text{and} \quad \sum_{s=1}^t w_s = 1.$$

Let  $G_{\lambda,t}(\bar{u}) = P_0(\bar{U}_{\lambda,t} \leq \bar{u})$  for  $\bar{u} \in [0, 1]$ . Then

$$F_{t,1}(\alpha) = G_{\lambda,t}\left(\frac{\alpha - (1 - \lambda)^t}{1 - (1 - \lambda)^t}\right).$$

For  $t \geq 2$ , the two largest weights are

$$w_t = \frac{\lambda}{1 - (1 - \lambda)^t} \quad \text{and} \quad w_{t-1} = \frac{\lambda(1 - \lambda)}{1 - (1 - \lambda)^t}.$$

Set

$$c = \frac{1}{w_t w_{t-1}} = \frac{(1 - (1 - \lambda)^t)^2}{\lambda^2(1 - \lambda)}.$$

If  $\epsilon \leq \min\{w_t, w_{t-1}\}$ , then the event  $\{\bar{U}_{\lambda,t} > 1 - \epsilon\}$  implies both  $\{w_t(1 - U_t) < \epsilon\}$  and  $\{w_{t-1}(1 - U_{t-1}) < \epsilon\}$ . By independence and the  $\text{Unif}(0, 1)$  CDF,

$$P_0(\bar{U}_{\lambda,t} > 1 - \epsilon) \leq \frac{\epsilon}{w_t} \cdot \frac{\epsilon}{w_{t-1}} = c\epsilon^2,$$

so

$$G_{\lambda,t}(1 - \epsilon) = 1 - P_0(\bar{U}_{\lambda,t} > 1 - \epsilon) \geq 1 - c\epsilon^2.$$

Choose

$$\epsilon^* = (1 - \eta) \min\left\{\frac{w_t}{2}, \frac{w_{t-1}}{2}, \frac{1 - (1 - \lambda)^t}{2c}\right\}, \quad \text{for some } \eta \in (0, 1).$$

Then  $\epsilon^* \leq \min\{w_t, w_{t-1}\}$  and  $c\epsilon^{*2} < \{1 - (1 - \lambda)^t\} \epsilon^*/2$ , yielding the chain of inequalities:

$$G_{\lambda,t}(1 - \epsilon^*) \geq 1 - c\epsilon^{*2} > 1 - \frac{1 - (1 - \lambda)^t}{2} \epsilon^* > 1 - (1 - (1 - \lambda)^t) \epsilon^*.$$

Setting  $\alpha^* = 1 - (1 - (1 - \lambda)^t) \epsilon^*$ , we conclude

$$F_{t,1}(\alpha^*) = G_{\lambda,t}(1 - \epsilon^*) > \alpha^*,$$

which violates the super-uniformity inequality  $P_0(\tilde{U}_{\lambda,t} \leq \alpha) \leq \alpha$  for all  $\alpha \in [0, 1]$ . Hence, for  $u_0 = 1$  and  $t \geq 2$ ,  $\tilde{U}_{\lambda,t}$  is not super-uniform.

We conclude this section with a positive outcome: although the process  $(\tilde{U}_{\lambda,t})_t$  is not globally super-uniform under  $H_0$ , it is left-tail super-uniform whenever  $u_0 \geq 1/2$ , i.e.,

$$P_0(\tilde{U}_{\lambda,t} \leq \alpha) \leq \alpha \text{ for every } \alpha \in [0, 1/2].$$

This enables us to still use  $(\tilde{U}_{\lambda,t})_t$  with the alarm rule  $\tilde{U}_{\lambda,t} \leq \alpha$  and still enjoy the guarantee of Proposition 1 (whose conclusion is valid for any fixed  $\alpha \in [0, 1]$  for which  $P_0(\tilde{U}_{\lambda,t} \leq \alpha) \leq \alpha$  for all  $t \geq 1$ ).

**Proposition 10.** *For each  $\alpha \in [0, 1/2]$ ,  $u_0 \geq 1/2$ ,  $\lambda \in (0, 1)$ , and  $t \geq 1$ ,*

$$P_0(\tilde{U}_{\lambda,t} \leq \alpha) \leq \alpha.$$

### 3 Directional and coordinate localisation via $p$ -value charts

We now specialise the framework to a setting where the monitored process is indexed by a  $d$ -dimensional parameter  $\theta = (\theta_1, \dots, \theta_d)$  with a fixed IC baseline  $\theta_0 = (\theta_{0,1}, \dots, \theta_{0,d}) \in \mathbb{R}^d$ . In a one-phase design, we may consider the null measure under  $H_0$ ,  $P_{X,0} = P_{X,\theta_0}$ , and test against the alternative that  $P_{X,t} = P_{X,\theta}$  for some  $\theta \neq \theta_0$ . In a two-phase design, for  $X \in \mathbb{R}^d$  one may assess the null  $H_0$  that  $P_{X,t} = P_{X,0}$  by testing, for example, the equality in mean  $EX_t = EX_0$ , where  $\Delta = EX_t - EX_0$  satisfies  $\Delta = 0$  under  $H_0$ .

At the point of alarm, our inferential objective is twofold: firstly, to identify affected coordinates  $j \in [d]$ , for which  $\theta_j \neq \theta_{0,j}$ . Secondly, for each affected coordinate  $j$ , to determine the direction of change, i.e., whether  $\theta_j < \theta_{0,j}$  or  $\theta_j > \theta_{0,j}$ . We aim to make these conclusions in a principled manner with simultaneous control, in the sense that the probability that at least one of our dimensional or directional conclusions is incorrect is bounded above by a pre-specified level  $\alpha$ .

To this end, for each coordinate  $j \in [d]$  and direction  $\square \in \{\leq, \geq\}$ , suppose we have a sequence of directional  $p$ -values  $(P_t^{(j,\square)})_{t \in \mathbb{N}}$  that test the corresponding one-sided null  $H_0^{(j,\square)}$  (e.g.,  $\theta_{0,j} \geq \theta_j$  when  $\square = \geq$ , or  $\theta_{0,j} \leq \theta_j$  when  $\square = \leq$ ). We assume that each sequence is valid in the super-uniform sense used in Section 2; i.e., for every  $t \in \mathbb{N}$  and  $\alpha \in [0, 1]$ ,

$$P_{0,t}^{(j,\square)}(P_t^{(j,\square)} \leq \alpha) \leq \alpha,$$

whenever  $P_{0,t}^{(j,\square)}$  is a probability measure on  $(\Omega, \mathfrak{A})$  such that the push-forward measures  $P_{X,s}$  satisfy  $H_0^{(j,\square)}$  for all  $s \in [t]$ . In particular, in a one-phase design the  $p$ -values may be of the form  $P_t^{(j,\square)} = p_t^{(j,\square)}(\mathbf{X}_1, \dots, \mathbf{X}_t)$  (or  $p_t^{(j,\square)}(\mathbf{X}_t)$ ), while in a two-phase design they may be of the form  $P_t^{(j,\square)} = p_t^{(j,\square)}(\mathbf{X}_0; \mathbf{X}_t)$ . When convenient, we may further assume the conditional super-uniformity property (as in (3)) with respect to a filtration  $(\mathcal{F}_t)_{t \in \mathbb{N}}$ .

Given these  $2d$  sequences of directional  $p$ -values, we construct an overall sequence of  $p$ -values

$(\bar{P}_t)_{t \in \mathbb{N}}$  satisfying the super-uniformity condition (1), and whose induced rejections satisfy the closed-testing principle of Marcus et al. (1976), based on the family of tests

$$\mathbb{H}_0 = \{H_0^{(j, \square)} : j \in [d], \square \in \{\leq, \geq\}\}.$$

Upon an alarm raised by the rule  $\bar{P}_t \leq \alpha$ , the procedure provides a set of rejections  $\mathbb{D}_t \subset [d] \times \{\leq, \geq\}$  such that the family-wise error rate satisfies

$$P_0(\exists (j, \square) \in \mathbb{D}_t : \theta_{0,j} \square \theta_j) \leq \alpha. \quad (9)$$

### 3.1 *p*-value chart construction

We take as input the  $2d$  sequences of *p*-values  $(P_t^{(j, \square)})_{t \in \mathbb{N}}$  and choose our level  $\alpha \in (0, 1)$  to determine our acceptable ARL. Then, at each time  $t$ , we proceed via the following steps:

1. For each  $j \in [d]$ , compute  $P_t^j = \min\{1, 2 \min\{P_t^{(j, \leq)}, P_t^{(j, \geq)}\}\}$ .
2. Compute the aggregate *p*-value via the expression  $\bar{P}_t = \min\{1, d \min_{j \in [d]} P_t^j\}$  or  $\bar{P}_t = \min\{1, \min\{2, d\} d^{-1} \sum_{j=1}^d P_t^j\}$ .

We then reject the global null hypothesis  $H_0 : \theta = \theta_0$  in favour of the alternative that  $\theta \neq \theta_0$  and raise an alarm at time  $t$  if  $\bar{P}_t \leq \alpha$ . Note that the two choices for  $\bar{P}_t$  correspond to the Bonferroni aggregator and the  $r = 1$  case of Lemma 5, with uniform weights to ensure that it satisfies the super-uniformity condition (1). One can instead compute the aggregate *p*-value via any other merging function that satisfies Lemma 5.

At the time point where we raise an alarm, we apply Holm's procedure (Holm, 1979) on the set  $\{P_t^j\}_{j \in [d]}$ . For each coordinate  $j$  that is rejected by Holm's procedure, we then place the pair  $(j, \leq)$  into  $\mathbb{D}_t$  if  $P_t^{(j, \leq)} \leq P_t^{(j, \geq)}$ , else we place the pair  $(j, \geq)$  into  $\mathbb{D}_t$ . The set of paired coordinates and directions  $\mathbb{D}_t$  then satisfies (9). We can summarise this process via the following steps:

1. Order  $\{P_t^j\}_{j \in [d]}$  to obtain the order statistics  $P_t^{(1)} \leq P_t^{(2)} \leq \dots \leq P_t^{(d)}$ , and note the corresponding indices of the ordering:  $j_{(1)}, \dots, j_{(d)}$ .
2. Let  $k^*$  be the largest  $k \in [d]$  such that  $P_t^{(i)} \leq \alpha/(d - i + 1)$  for all  $i \in [k]$ . Put  $j_{(1)}, \dots, j_{(k^*)}$  into  $\mathbb{J}_t$ .
3. For each  $j \in \mathbb{J}_t$ , if  $P_t^{(j, \leq)} \leq P_t^{(j, \geq)}$ , then put  $(j, \leq)$  into  $\mathbb{D}_t$ ; else, put  $(j, \geq)$  into  $\mathbb{D}_t$ .

#### 3.1.1 Family-wise error rate control

To verify that (9) holds, we first recall the closed testing principle of Marcus et al. (1976) (see also Dickhaus, 2014, Thm. 3.4) and the equivalence of Holm's step-down procedure to the Bonferroni closure (cf. Holm, 1979).

**Theorem 11.** Let  $\{\mathbb{H}_j : j \in [m]\}$  be a finite family of hypotheses. For every nonempty  $\mathbb{J} \subseteq [m]$ , write  $\mathbb{H}_{\mathbb{J}} = \bigcap_{j \in \mathbb{J}} \mathbb{H}_j$  and let  $\mathcal{M}(\mathbb{H}_{\mathbb{J}})$  denote the set of all data-generating distributions under  $\mathbb{H}_{\mathbb{J}}$ . Suppose that for each such  $\mathbb{J}$  we are given a local test  $T_{\mathbb{J}}$  of  $\mathbb{H}_{\mathbb{J}}$  with level  $\alpha$  in the sense that

$$\sup_{Q \in \mathcal{M}(\mathbb{H}_{\mathbb{J}})} Q(T_{\mathbb{J}} = 1) \leq \alpha.$$

Define the closed testing procedure that rejects an elementary hypothesis  $\mathbb{H}_j$  if and only if  $T_{\mathbb{J}}$  rejects  $\mathbb{H}_{\mathbb{J}}$  for every  $\mathbb{J}$  such that  $j \in \mathbb{J}$ . Then the procedure has strong FWER control at level  $\alpha$ , i.e.

$$Q(\exists j \in [m] \text{ with } \mathbb{H}_j \text{ true and rejected}) \leq \alpha,$$

for any data-generating distribution  $Q$ .

**Theorem 12.** Let  $\{P_j\}_{j \in [m]}$  be super-uniform  $p$ -values for the hypotheses  $\{\mathbb{H}_j\}_{j \in [m]}$ . For each nonempty  $\mathbb{J} \subset [m]$ , define the Bonferroni local test:

$$T_{\mathbb{J}}^{\text{Bon}} = \mathbf{1}_{\{\min_{j \in \mathbb{J}} P_j \leq \alpha/|\mathbb{J}|\}}.$$

Then the closed testing procedure generated by  $\{T_{\mathbb{J}}^{\text{Bon}}\}_{\mathbb{J} \subset [m]}$  is exactly Holm's step-down procedure: i.e., if  $P_{(1)} \leq \dots \leq P_{(m)}$  are order statistics of  $\{P_j\}_{j \in [m]}$ , with indices  $j_{(1)}, \dots, j_{(m)}$ , then reject  $\mathbb{H}_{j_{(1)}}, \dots, \mathbb{H}_{j_{(k^*)}}$ , where  $k^*$  is the largest  $k \in [m]$  such that  $P_{(i)} \leq \alpha/(m-i+1)$  for all  $i \in [k]$ .

We now proceed to prove that (9) holds. For each fixed  $t \in \mathbb{N}$ , coordinate  $j \in [d]$  and direction  $\square \in \{\leq, \geq\}$ , we recall that the  $p$ -value  $P_t^{(j, \square)}$  is super-uniform under the null  $H_0^{(j, \square)}$ . Let  $P_{0,t}^j$  be a probability measure on  $(\Omega, \mathfrak{A})$  such that the push-forward measures  $P_{X,s}$  satisfy  $H_0^j : \theta_j = \theta_{0,j}$  for all  $s \in [t]$ . Then  $P_{0,t}^j(P_t^j \leq \alpha) \leq \alpha$ , for every  $\alpha \in [0, 1]$ . To see this, observe that

$$P_{0,t}^j(2 \min\{P_t^{(j, \leq)}, P_t^{(j, \geq)}\} \leq \alpha) \leq P_{0,t}^j(P_t^{(j, \leq)} \leq \alpha/2) + P_{0,t}^j(P_t^{(j, \geq)} \leq \alpha/2) \leq \alpha, \quad (10)$$

via the union bound and super-uniformity of the  $p$ -values. The validity of our directional procedure is then stated as follows.

**Proposition 13.** The procedure from Section 3.1 satisfies (9) at each time  $t \in \mathbb{N}$ .

While preparing this manuscript, we became aware that the procedure in Section 3.1 is a special case of the simultaneous directional inference framework of Heller & Solari (2024). This observation suggests that broader classes of localisation-type charts, beyond our proposal, can be developed along the same lines.

Table 1: Average  $R_k$  versus  $k$ -ARL bounds from Proposition 3 for two-phase normal example  $p$ -value charts, with 100 simulation repetitions.

$\alpha$	$k$	mean $R_k$	st. err. $R_k$	lower bound	ratio
0.01	1	1206.47	204.01	50.5	23.89
0.01	5	5255.38	592.48	250.5	20.98
0.05	1	74.4	12.29	10.5	7.09
0.05	5	316.37	33.12	50.5	6.26

## 4 Example applications

We demonstrate the correctness of our theory and the usefulness of our results through the following examples and simulations. All R scripts for these simulations are available at [https://github.com/hiendn/Pvalue\\_SPC](https://github.com/hiendn/Pvalue_SPC).

### 4.1 Elementary examples

We start by considering the one-phase design where we operate under the global assumption that  $X$  is normally distributed with law  $N(\mu, \sigma^2)$ , for some  $\mu \in \mathbb{R}$  and  $\sigma^2 > 0$ . If we consider a one-phase design where we take  $H_0$  to be the hypothesis that  $X \sim N(0, 1)$  and observe a single observation  $X_t$  at each time  $t$ , where  $(X_t)_t$  is an IID sequence, then the natural test statistic is  $Z_t = X_t$ . By the probability integral transform and our observation about the tightness of the bound  $E_0 R \geq 1/\alpha$ , it follows that we can exactly control the  $k$ -ARL for this procedure at level  $k/\alpha$  by raising an alarm whenever  $|Z_t| \geq \zeta_{1-\alpha/2}$ , where  $\zeta_u$  is the  $u$ th quantile of the standard normal distribution. However, in this scenario, the  $p$ -value for  $H_0$  is exactly  $P_t = 2\{1 - \Phi(|X_t|)\}$  (satisfying (3)), where  $\Phi$  is the standard normal CDF, which yields exactly the same decision rule if we raise an alarm whenever  $P_t \leq \alpha$ , and thus in this elementary example, the chart based on either the sequence  $(P_t)_t$  or  $(Z_t)_t$  will perform exactly the same.

We note that we can similarly propose an elementary two-phase design, whereupon in Phase I, we observe a single observation  $X_0 \sim N(\mu_0, 1)$  and in Phase II we observe  $X_t \sim N(\mu_1, 1)$  at each time  $t$ , where  $(X_t)_t$  is an IID sequence. To test the hypothesis  $H_0 : \mu_0 = \mu_1$  at each time  $t$ , we can use the test statistic  $Z_t = (X_t - X_0)/\sqrt{2}$  and raise an alarm whenever  $|Z_t| \geq \zeta_{1-\alpha/2}$ . Equivalently, we can compute the  $p$ -value  $P_t = 2\{1 - \Phi(|Z_t|)\}$  and raise an alarm under the usual rule that  $P_t \leq \alpha$ . In the one-phase IID case above, the  $k$ -ARL is controlled at exactly  $k/\alpha$ . However, in the present two-phase baseline-with-reuse setting, the  $p$ -values are (unconditionally) super-uniform but  $Z_t$  is not independent of  $\mathcal{F}_{t-1}$ , so (3) need not hold and exact equality at  $k/\alpha$  need not occur. To assess the tightness of the bounds from Propositions 1 and 3 for  $(P_t)_t$  in this setting, we consider a short simulation using alarm rules with  $\alpha \in \{0.01, 0.05\}$  assessing the  $k$ -ARL for  $k \in \{1, 5\}$ . We conduct 100 repetitions for each setting and report the results in Table 1.

Let us consider a slightly less elementary two-phase design where in Phase I, we observe  $X_0 \sim$

$N(0, 1)$ , and in Phase II, we observe the autoregressive data  $X_t = \delta + \beta X_{t-1} + \varepsilon_t$ , where  $\varepsilon_t \sim N(0, \sigma^2)$ ,  $|\beta| < 1$  and  $\sigma^2 = 1 - \beta^2$  (i.e., the process  $(X_t)_t$  is stationary with marginal law  $X_t \sim N(\delta/(1-\beta), 1)$ ). Here,  $\beta \neq 0$  is unknown. In this situation  $X_t$  is not independent of the history  $\mathcal{F}_{t-1} = \sigma(X_0, \dots, X_{t-1})$ . Naturally, to test the null  $H_0 : \delta = 0$ , we can use the marginal test statistics  $Z_t = X_t$ , which generate the  $p$ -values  $P'_t = 2\{1 - \Phi(|X_t|)\}$ , which satisfy (1) but not (3), and thus only the bounds of Propositions 1 and 3 apply.

Alternatively, consider that when  $\beta$  is known to equal  $b \in (-1, 1)$ , we can take  $Z_t(b) = \{X_t - bX_{t-1}\} / \sqrt{1 - b^2}$ , and compute its  $p$ -value as  $P_t(b) = 2\{1 - \Phi(|Z_t(b)|)\}$ . Indeed, if  $\beta = b$ , then under  $H_0$ , conditional on  $\mathcal{F}_{t-1}$ ,  $X_t \sim N(bX_{t-1}, 1 - b^2)$ . However, since  $\beta$  is not known, we can instead compute  $P_t^* = \sup_{b \in (-1, 1)} P_t(b)$ , and note that since  $P_t^* \geq P_t(\beta)$  and  $P_t(\beta) | \mathcal{F}_{t-1} \sim \text{Unif}(0, 1)$ , it holds that  $P_0(P_t^* \leq \alpha | \mathcal{F}_{t-1}) \leq \alpha$ , for each  $\alpha \in [0, 1]$ , and thus satisfies (3) (cf. Berger & Boos, 1994). In fact, we have the closed form  $P_t^* = 2\left\{1 - \Phi\left(\sqrt{[X_t^2 - X_{t-1}^2]_+}\right)\right\}$ , since, over  $(-1, 1)$ , the function  $g(b) = (y - bx)^2 / (1 - b^2)$  achieves its minimum at  $b = y/x$  when  $|y| \leq |x|$ , yielding value 0, and at the unique stationary point  $b = x/y$  otherwise, yielding value  $y^2 - x^2$ ; thus  $\inf_{b \in (-1, 1)} \sqrt{g(b)} = \sqrt{[y^2 - x^2]_+}$ . We conclude that the sequence  $(P_t^*)_t$  satisfies (3) but is not generated by a probability integral transformation and thus the bounds of Propositions 2 and 4 apply but may not be tight.

To assess the  $k$ -ARL performance of the two charts  $(P'_t)_t$  and  $(P_t^*)_t$  and the tightness of the theoretical bounds, we simulate the  $k$ -ARL values of both charts for the scenario where  $\beta \in \{0.1, 0.5\}$ , under the null hypothesis (i.e.,  $\delta = 0$ ), for alarm rules based on  $\alpha \in \{0.01, 0.05\}$  and  $k \in \{1, 5\}$ . We conduct 100 repetitions of each scenario and report the results in Table 2.

## 4.2 Kolmogorov–Smirnov-based EWMA charts

We now consider a two-phase setting for EWMA charts, whereby in Phase I one observes IID data  $\mathbf{X}_0 = (X_{0,i})_{i=1}^{n_0}$  of sample size  $n_0$ , where each  $X_{0,i}$  is a replicate of  $X_0 : \Omega \rightarrow \mathbb{R}$  with probability measure  $P_{X,0}$ . Then, in Phase II, we monitor data sets  $\mathbf{X}_t = (X_{t,i})_{i=1}^{n_t}$  of sizes  $n_t \in \mathbb{N}$ , corresponding to a VSS setting. Here, the process is in control (IC) at time  $t$  if the null hypothesis that  $P_{X,s} = P_{X,0}$  for all  $s \in [t]$  holds, and out of control (OOC) otherwise. At time  $t$ , we test  $H_0 : P_{X,t} = P_{X,0}$  using the classical two-sample Kolmogorov–Smirnov (KS) test statistic, where

$$Z_t = \sup_{x \in \mathbb{R}} |F_{0,n_0}(x) - F_{t,n_t}(x)|,$$

with  $F_{0,n_0}(x) = n_0^{-1} \sum_{i=1}^{n_0} \mathbf{1}_{(-\infty, x]}(X_{0,i})$  and  $F_{t,n_t}(x) = n_t^{-1} \sum_{i=1}^{n_t} \mathbf{1}_{(-\infty, x]}(X_{t,i})$  the empirical CDFs of  $\mathbf{X}_0$  and  $\mathbf{X}_t$ , respectively. The KS test statistic has a well-known finite-sample distribution under the null hypothesis and thus we can compute a sequence of  $p$ -values  $(P_t)_t$  using standard implementations such as the `ks.test()` function in R (see e.g., Nikiforov, 1994 and cf. Gibbons & Chakraborti, 2010, Sec. 6.3).

Table 2: Average  $R_k$  versus  $k$ -ARL bounds from Propositions 3 and 4 for autoregressive example  $p$ -value charts  $(P'_t)_t$  and  $(P^*_t)_t$ , respectively, with 100 simulation repetitions.

Chart	$\beta$	$\alpha$	$k$	mean $R_k$	st. err. $R_k$	lower bound	ratio
$(P'_t)_t$	0.1	0.01	1	84.93	8.17	50.5	1.68
	0.1	0.01	5	453.21	21.20	250.5	1.81
	0.1	0.05	1	22.6	2.03	10.5	2.15
	0.1	0.05	5	93.61	3.63	50.5	1.85
	0.5	0.01	1	119.79	13.65	50.5	2.37
	0.5	0.01	5	502.01	24.31	250.5	2.00
	0.5	0.05	1	22.54	2.06	10.5	2.15
	0.5	0.05	5	112.04	5.37	50.5	2.22
$(P^*_t)_t$	0.1	0.01	1	123.77	13.23	100	1.24
	0.1	0.01	5	718.19	37.09	500	1.44
	0.1	0.05	1	30.26	2.71	20	1.51
	0.1	0.05	5	135.94	5.20	100	1.36
	0.5	0.01	1	279.61	29.07	100	2.80
	0.5	0.01	5	1311.44	59.53	500	2.62
	0.5	0.05	1	38.97	3.20	20	1.95
	0.5	0.05	5	222.31	8.60	100	2.22

We note that the sequence  $(P_t)_t$  satisfies the super-uniformity condition (1). Thus, if we raise an alarm whenever  $P_t \leq \alpha$ , Proposition 3 implies that we should expect the  $k$ -ARL values to be bounded below by  $k/(2\alpha) + 1/2$  for each  $k \geq 1$ . To assess the tightness of this bound, we simulate the following setting. We let  $n_0 \in \{20, 50, 100\}$ ,  $n_t = N_t \sim \text{DiscUnif}[n_0 - 10, n_0 + 10]$ ,  $\alpha \in \{0.01, 0.05\}$ ,  $k \in \{1, 5\}$  and take  $X_0 \sim N(0, 1)$ . Here, we note that the distribution of the KS test statistic under a continuous null distribution is the same for all choices and thus any continuous distribution on  $X_0$  will yield the same simulation outcomes. The resulting average times to first  $k$  alarms  $R_k$  from 100 replications of each scenario are provided in Table 3.

Next, to assess the correctness of Propositions 6 and 7 we consider the application of the charts  $(\tilde{Q}_{\lambda,t}^{(r)})_t$  and  $(\bar{Q}_{\lambda,t}^{(r)})_t$  from Section 2.4.1, using the base sequence  $(P_t)_t$ . We take  $n_0 \in \{50, 100, 200\}$  and  $n_t$  as above, and we assess the cases when  $\alpha \in \{0.05, 0.1\}$ ,  $k \in \{1, 5\}$ , and  $X_0 \sim N(0, 1)$ . For  $(\tilde{Q}_{\lambda,t}^{(r)})_t$  we choose  $\lambda = 1/2$  and  $r \in \{-0.9, -0.8\}$ , while for  $(\bar{Q}_{\lambda,t}^{(r)})_t$  we consider  $\lambda \in \{0.8, 0.9\}$  and  $r = 1$ . The average  $R_k$  values from 100 replications of each setting are provided in Tables 4 and 9.

To obtain some insights regarding the performance of these charts for detecting OOC processes, we will consider again taking  $n_0 \in \{50, 100, 200\}$ , with  $n_t$  as in Table 3. We assess the performance of the raw  $(P_t)_t$  sequence, along with the charts  $(\tilde{Q}_{\lambda,t}^{(r)})_t$  and  $(\bar{Q}_{\lambda,t}^{(r)})_t$ . Here we consider alarm rules based on  $\alpha \in \{0.01, 0.05\}$ , where  $X_0 \sim N(0, 1)$  but we take two settings for the OOC  $X_t$ . In the first case the process is persistently OOC in the sense that  $X_t$  is distributed as  $N(1/2, 1)$ ,  $N(1, 1)$ ,  $N(0, 2)$ , and Cauchy for every  $t \in \mathbb{N}$ . In the second case, the process is OOC with  $X_t$  distributed dynamically as  $N(\mu_t, 1)$  or  $N(0, \sigma_t^2)$ , where  $\mu_t \sim N(0, 1/2)$  or  $\mu_t \sim N(0, 1/4)$ , and  $\sigma_t^2 \sim \chi_1^2$  or  $\sigma_t^2 \sim \chi_2^2$ . For  $(\tilde{Q}_{\lambda,t}^{(r)})_t$  we choose  $\lambda = 1/2$  and  $r \in \{-0.9, -0.8\}$ , while for  $(\bar{Q}_{\lambda,t}^{(r)})_t$  we consider

Table 3: Average  $R_k$  versus  $k$ -ARL bounds from Proposition 3 for KS test statistic  $p$ -value charts  $(P_t)_t$ , using 100 simulation repetitions.

$n_0$	$\alpha$	$k$	mean $R_k$	st. err. $R_k$	lower bound	ratio
20	0.01	1	1318.30	307.79	50.5	26.10
20	0.01	5	7822.24	1136.65	250.5	31.23
20	0.05	1	68.38	13.19	10.5	6.51
20	0.05	5	410.77	54.22	50.5	8.13
50	0.01	1	1465.94	288.67	50.5	29.03
50	0.01	5	5672.49	818.32	250.5	22.64
50	0.05	1	85.55	15.01	10.5	8.15
50	0.05	5	397.58	41.43	50.5	7.87
100	0.01	1	1663.56	316.09	50.5	32.94
100	0.01	5	4005.76	610.87	250.5	15.99
100	0.05	1	68.63	10.41	10.5	6.54
100	0.05	5	394.16	41.78	50.5	7.81

Table 4: Average  $R_k$  while IC versus  $k$ -ARL bounds from Proposition 3 for KS EWMA-like  $p$ -value charts  $(\tilde{Q}_{\lambda,t}^{(r)})_t$  and  $(\bar{Q}_{\lambda,t}^{(r)})_t$ , using 100 simulation repetitions. This table contains results for  $n_0 = 50$ , while Appendix Table 9 contains results for  $n_0 \in \{100, 200\}$ .

Chart	$n_0$	$\alpha$	$k$	$\lambda$	$r$	mean $R_k$	st. err. $R_k$	lower bound	ratio
$\tilde{Q}_{\lambda,t}^{(r)}$	50	0.05	1	0.5	-0.9	32846.69	7587.56	10.5	3128.2562
	50	0.05	1	0.5	-0.8	12091.79	3184.22	10.5	1151.5990
	50	0.05	5	0.5	-0.9	75643.87	14807.62	50.5	1497.8984
	50	0.05	5	0.5	-0.8	36112.13	5902.91	50.5	715.0917
	50	0.1	1	0.5	-0.9	7334.45	1907.45	5.5	1333.5364
	50	0.1	1	0.5	-0.8	2566.96	588.93	5.5	466.72
	50	0.1	5	0.5	-0.9	35103.81	9423.84	25.5	1376.62
	50	0.1	5	0.5	-0.8	12640.32	2615.45	25.5	495.6988
$\bar{Q}_{\lambda,t}^{(r)}$	50	0.05	1	0.9	1	2005.07	515.08	10.5	190.9590
	50	0.05	1	0.95	1	192.31	27.32	10.5	18.3152
	50	0.05	5	0.9	1	6851.53	1628.88	50.5	135.6739
	50	0.05	5	0.95	1	1417.72	261.55	50.5	28.0737
	50	0.1	1	0.9	1	111.16	18.43	5.5	20.2109
	50	0.1	1	0.95	1	44.14	7.03	5.5	8.0255
	50	0.1	5	0.9	1	480.42	73.81	25.5	18.84
	50	0.1	5	0.95	1	222.61	24.91	25.5	8.7298

$\lambda \in \{0.8, 0.9\}$  and  $r = 1$ . To assess the relative performances, we compute the average time to the first  $k$  alarms  $R_k$  for  $k \in \{1, 5\}$  from 100 replicates and report the persistent OOC outcomes in Tables 5, 10 and 11, and the dynamic OOC outcomes in Tables 6, 12, and 13.

Finally we note that we are not the first to consider the use of KS tests in the SPC literature, and our work is preceded by the texts of Bakir (2012), Ross & Adams (2012), Ross (2015), and Khrueasom & Pongpullponsak (2016). In particular, we note that Ross & Adams (2012) use the asymptotic distribution of the KS statistic to deduce a comprehensive table of time-dependent thresholds for SPC via normalised forms of KS statistics  $(Z_t)_t$  for calibrating charts to achieve some specific ARL values. These dynamic thresholds were then implemented in the R package `cpm` in Ross (2015). ARL estimation is also performed in Khrueasom & Pongpullponsak (2016) for one-sample KS charts using the fact that the empirical CDF multiplied by  $n$  is binomial pointwise, although the use of this fact is not made theoretically rigorous. Lastly, in these previous works, there is no treatment of EWMA or EWMA-like charts based on KS statistics, nor are general formulas available for control of the ARL or  $k$ -ARL under fixed alarm rules, for finite  $n_0$  and  $(n_t)_t$ .

### 4.3 The distribution of uniform EWMA charts

To assess the veracity of the theory from Section 2.4.2, we simulate 10000 replicates of the random variable  $\tilde{U}_{\lambda,t}$  for  $\lambda \in \{0.3, 0.5, 0.7\}$  up to times  $t \in \{2, 3, 4\}$ , taking  $u_0 = 1/2$  in every case. Histograms for each of the  $(t, \lambda)$  combinations are plotted and displayed against the corresponding theoretical PDF for the statistic  $\tilde{U}_{\lambda,t}$  as predicted by Proposition 9 in Figure 1. Furthermore, we demonstrate that for each of the scenarios above, the statistic  $\tilde{U}_{\lambda,t}$  is left-tail super-uniform as predicted by Proposition 10 by plotting the CDFs against that of the uniform distribution, in Figure 2.

### 4.4 Directional and coordinate localisation charts

To demonstrate the results of Section 3.1, we consider a pair of examples. In the first case, we consider a one-phase setting where  $X_0 \sim N(0, \Sigma)$  is a  $d = 3$  dimensional normal random vector with  $\Sigma = (\Sigma_{jk})_{j,k \in [d]}$ , where  $\Sigma_{jj} = 1$  for each  $j \in [d]$  and  $\Sigma_{jk} = \rho > 0$  for  $j \neq k$ . For each time point  $t \in \mathbb{N}$ , we observe the OOC random variable  $X_t \sim N(\mu, \Sigma)$ , where  $\mu = (\delta, 0, -\delta)$  for  $\delta > 0$ . Noting that for each  $t$  and  $j$ ,  $Z_{t,j} = X_{t,j}/\sqrt{\Sigma_{jj}} \sim N(0, 1)$  under the IC hypothesis, we can implement the method from Section 3.1 via the  $p$ -value sequences  $(P_t^{(j,\square)})_t$ , where  $P_t^{(j,\geq)} = 1 - \Phi(Z_{t,j})$  and  $P_t^{(j,\leq)} = \Phi(Z_{t,j})$ , and combinations are obtained via the Bonferroni rule. We assess the power of our directional and coordinate localisation charts via implementation with control limits  $\alpha \in \{0.01, 0.05\}$ , and consider scenarios  $\delta \in \{0.5, 1\}$  and  $\rho \in \{0, 0.5, 0.9\}$ . To assess the power, we conduct 100 replications of simulation runs whereupon we compute the average run times  $R$ , and the number of detected OOC directions ( $\#\text{OOC}$ ; i.e., whether both OOC directions are detected,

Table 5: Average  $R_k$  under persistent OOC processes for KS  $p$ -value charts  $(P_t)_t$ ,  $\left(\tilde{Q}_{\lambda,t}^{(r)}\right)_t$  and  $\left(\bar{Q}_{\lambda,t}^{(r)}\right)_t$ , using 100 simulation repetitions. This table contains results for  $n_0 = 50$ , while Appendix Tables 10 and 11 contains results for  $n_0 = 100$  and  $n_0 = 200$ , respectively.

OOC process	$n_0$	$\alpha$	Chart	$r$	$\lambda$	mean $R_1$	st. err. $R_1$	mean $R_5$	st. err. $R_5$	
N(1/2, 1)	50	0.01	$P_t$			36.06	23.53	185.58	90.08	
	50	0.01	$\tilde{Q}_{\lambda,t}^{(r)}$	-0.9	0.5	692.27	300.34	3515.62	1359.13	
	50	0.01	$\tilde{Q}_{\lambda,t}^{(r)}$	-0.8	0.5	1707.76	1346.76	3517.78	2157.76	
	50	0.01	$\tilde{Q}_{\lambda,t}^{(r)}$	1	0.9	54842.44	54471.80	252708.58	250810.10	
	50	0.01	$\bar{Q}_{\lambda,t}^{(r)}$	1	0.95	759.31	488.57	4318.98	3164.00	
	50	0.05	$P_t$			3.25	0.56	13.33	1.76	
	50	0.05	$\tilde{Q}_{\lambda,t}^{(r)}$	-0.9	0.5	85.23	37.17	305.66	101.19	
	50	0.05	$\tilde{Q}_{\lambda,t}^{(r)}$	-0.8	0.5	125.01	65.85	351.70	158.42	
	50	0.05	$\bar{Q}_{\lambda,t}^{(r)}$	1	0.9	5.78	1.87	27.35	8.29	
	50	0.05	$\bar{Q}_{\lambda,t}^{(r)}$	1	0.95	5.38	1.64	26.12	7.81	
	N(1, 1)	50	0.01	$P_t$		1.10	0.04	5.27	0.08	
		50	0.01	$\tilde{Q}_{\lambda,t}^{(r)}$	-0.9	0.5	1.53	0.22	6.15	0.75
		50	0.01	$\tilde{Q}_{\lambda,t}^{(r)}$	-0.8	0.5	1.24	0.06	5.55	0.17
		50	0.01	$\bar{Q}_{\lambda,t}^{(r)}$	1	0.9	1.14	0.09	5.62	0.27
		50	0.01	$\bar{Q}_{\lambda,t}^{(r)}$	1	0.95	1.07	0.03	5.27	0.06
		50	0.05	$P_t$		1.00	0.00	5.04	0.02	
		50	0.05	$\tilde{Q}_{\lambda,t}^{(r)}$	-0.9	0.5	1.07	0.04	5.15	0.08
		50	0.05	$\tilde{Q}_{\lambda,t}^{(r)}$	-0.8	0.5	1.07	0.04	5.09	0.04
		50	0.05	$\bar{Q}_{\lambda,t}^{(r)}$	1	0.9	1.00	0.00	5.01	0.01
		50	0.05	$\bar{Q}_{\lambda,t}^{(r)}$	1	0.95	1.04	0.02	5.08	0.04
N(0, 2)	50	0.01	$P_t$			373.91	142.99	1197.07	308.02	
	50	0.01	$\tilde{Q}_{\lambda,t}^{(r)}$	-0.9	0.5	36498.91	13402.09	122395.82	28771.52	
	50	0.01	$\tilde{Q}_{\lambda,t}^{(r)}$	-0.8	0.5	13889.67	4649.08	104257.62	68852.89	
	50	0.01	$\bar{Q}_{\lambda,t}^{(r)}$	1	0.9	120454.57	59829.87	1047349.86	528364.60	
	50	0.01	$\bar{Q}_{\lambda,t}^{(r)}$	1	0.95	3955.17	2125.32	18878.65	6016.02	
	50	0.05	$P_t$			19.31	4.05	89.55	10.52	
	50	0.05	$\tilde{Q}_{\lambda,t}^{(r)}$	-0.9	0.5	1549.00	441.42	6552.55	1558.61	
	50	0.05	$\tilde{Q}_{\lambda,t}^{(r)}$	-0.8	0.5	493.85	81.41	3406.35	561.96	
	50	0.05	$\bar{Q}_{\lambda,t}^{(r)}$	1	0.9	143.39	44.38	520.81	132.94	
	50	0.05	$\bar{Q}_{\lambda,t}^{(r)}$	1	0.95	35.93	6.71	178.34	23.72	
	Cauchy	50	0.01	$P_t$		59.00	8.73	420.38	55.63	
		50	0.01	$\tilde{Q}_{\lambda,t}^{(r)}$	-0.9	0.5	7138.85	1220.77	28983.64	4323.72
		50	0.01	$\tilde{Q}_{\lambda,t}^{(r)}$	-0.8	0.5	5510.04	1460.69	23253.50	5417.67
		50	0.01	$\bar{Q}_{\lambda,t}^{(r)}$	1	0.9	7362.64	2945.71	42590.51	17517.25
		50	0.01	$\bar{Q}_{\lambda,t}^{(r)}$	1	0.95	1877.77	562.83	5772.51	1262.26
		50	0.05	$P_t$		10.92	1.56	46.41	4.18	
		50	0.05	$\tilde{Q}_{\lambda,t}^{(r)}$	-0.9	0.5	704.47	94.75	3067.70	397.01
		50	0.05	$\tilde{Q}_{\lambda,t}^{(r)}$	-0.8	0.5	331.04	41.87	1206.27	144.66
		50	0.05	$\bar{Q}_{\lambda,t}^{(r)}$	1	0.9	34.00	6.69	134.56	19.90
		50	0.05	$\bar{Q}_{\lambda,t}^{(r)}$	1	0.95	13.20	2.09	73.73	9.92

Table 6: Average  $R_k$  under dynamic OOC processes for KS  $p$ -value charts  $(P_t)_t$ ,  $\left(\tilde{Q}_{\lambda,t}^{(r)}\right)_t$  and  $\left(\bar{Q}_{\lambda,t}^{(r)}\right)_t$ , using 100 simulation repetitions. This table contains results for  $n_0 = 50$ , while Appendix Tables 12 and 13 contains results for  $n_0 = 100$  and  $n_0 = 200$ , respectively.

OOC process	$n_0$	$\alpha$	Chart	$r$	$\lambda$	mean $R_1$	st. err. $R_1$	mean $R_5$	st. err. $R_5$
$N(\mu_t, 1)$	50	0.01	$P_t$			2.58	0.22	12.39	0.46
	$\mu_t \sim N(0, 1/2)$	50	$\tilde{Q}_{\lambda,t}^{(r)}$	-0.9	0.5	4.32	0.42	9.14	0.48
		50	$\tilde{Q}_{\lambda,t}^{(r)}$	-0.8	0.5	3.29	0.30	8.39	0.42
		50	$\tilde{Q}_{\lambda,t}^{(r)}$	1	0.9	4.83	0.56	25.04	1.50
		50	$\bar{Q}_{\lambda,t}^{(r)}$	1	0.95	3.55	0.39	20.24	0.99
		50	$P_t$			1.91	0.17	9.37	0.29
		50	$\tilde{Q}_{\lambda,t}^{(r)}$	-0.9	0.5	3.10	0.28	7.68	0.36
		50	$\tilde{Q}_{\lambda,t}^{(r)}$	-0.8	0.5	2.33	0.17	6.76	0.20
		50	$\bar{Q}_{\lambda,t}^{(r)}$	1	0.9	2.22	0.18	11.65	0.49
		50	$\bar{Q}_{\lambda,t}^{(r)}$	1	0.95	1.83	0.12	10.65	0.44
$N(\mu_t, 1)$	50	0.01	$P_t$			3.98	0.33	19.18	0.86
	$\mu_t \sim N(0, 1/4)$	50	$\tilde{Q}_{\lambda,t}^{(r)}$	-0.9	0.5	9.82	1.48	19.16	1.84
		50	$\tilde{Q}_{\lambda,t}^{(r)}$	-0.8	0.5	7.26	0.74	17.95	1.42
		50	$\tilde{Q}_{\lambda,t}^{(r)}$	1	0.9	10.58	1.27	52.62	2.71
		50	$\bar{Q}_{\lambda,t}^{(r)}$	1	0.95	7.66	0.84	39.93	2.40
		50	$P_t$			2.50	0.20	12.77	0.43
		50	$\tilde{Q}_{\lambda,t}^{(r)}$	-0.9	0.5	5.23	0.45	11.70	0.80
		50	$\tilde{Q}_{\lambda,t}^{(r)}$	-0.8	0.5	4.61	0.49	11.96	0.85
		50	$\bar{Q}_{\lambda,t}^{(r)}$	1	0.9	3.40	0.36	18.10	0.83
		50	$\bar{Q}_{\lambda,t}^{(r)}$	1	0.95	2.90	0.28	14.36	0.57
$N(\mu_t, 1)$	50	0.01	$P_t$			3.61	0.35	18.02	0.82
	$\sigma_t^2 \sim \chi_1^2$	50	$\tilde{Q}_{\lambda,t}^{(r)}$	-0.9	0.5	6.17	0.71	13.43	1.00
		50	$\tilde{Q}_{\lambda,t}^{(r)}$	-0.8	0.5	6.15	0.72	12.85	1.16
		50	$\bar{Q}_{\lambda,t}^{(r)}$	1	0.9	9.62	1.07	48.12	3.59
		50	$\bar{Q}_{\lambda,t}^{(r)}$	1	0.95	6.52	0.72	30.31	1.75
		50	$P_t$			2.07	0.21	11.68	0.46
		50	$\tilde{Q}_{\lambda,t}^{(r)}$	-0.9	0.5	4.20	0.40	10.49	0.67
		50	$\tilde{Q}_{\lambda,t}^{(r)}$	-0.8	0.5	3.60	0.34	8.59	0.49
		50	$\bar{Q}_{\lambda,t}^{(r)}$	1	0.9	3.06	0.26	16.18	0.81
		50	$\bar{Q}_{\lambda,t}^{(r)}$	1	0.95	2.48	0.22	13.23	0.64
$N(\mu_t, 1)$	50	0.01	$P_t$			8.10	0.80	38.57	1.91
	$\sigma_t^2 \sim \chi_2^2$	50	$\tilde{Q}_{\lambda,t}^{(r)}$	-0.9	0.5	47.59	5.25	113.35	13.21
		50	$\tilde{Q}_{\lambda,t}^{(r)}$	-0.8	0.5	30.55	3.66	76.98	7.22
		50	$\bar{Q}_{\lambda,t}^{(r)}$	1	0.9	55.59	8.91	254.77	24.81
		50	$\bar{Q}_{\lambda,t}^{(r)}$	1	0.95	21.14	2.57	103.50	6.81
		50	$P_t$			3.14	0.24	18.04	0.88
		50	$\tilde{Q}_{\lambda,t}^{(r)}$	-0.9	0.5	18.31	1.95	39.48	3.10
		50	$\tilde{Q}_{\lambda,t}^{(r)}$	-0.8	0.5	15.54	1.65	32.88	2.91
		50	$\bar{Q}_{\lambda,t}^{(r)}$	1	0.9	4.23	0.45	27.51	1.62
		50	$\bar{Q}_{\lambda,t}^{(r)}$	1	0.95	4.07	0.45	22.92	1.29

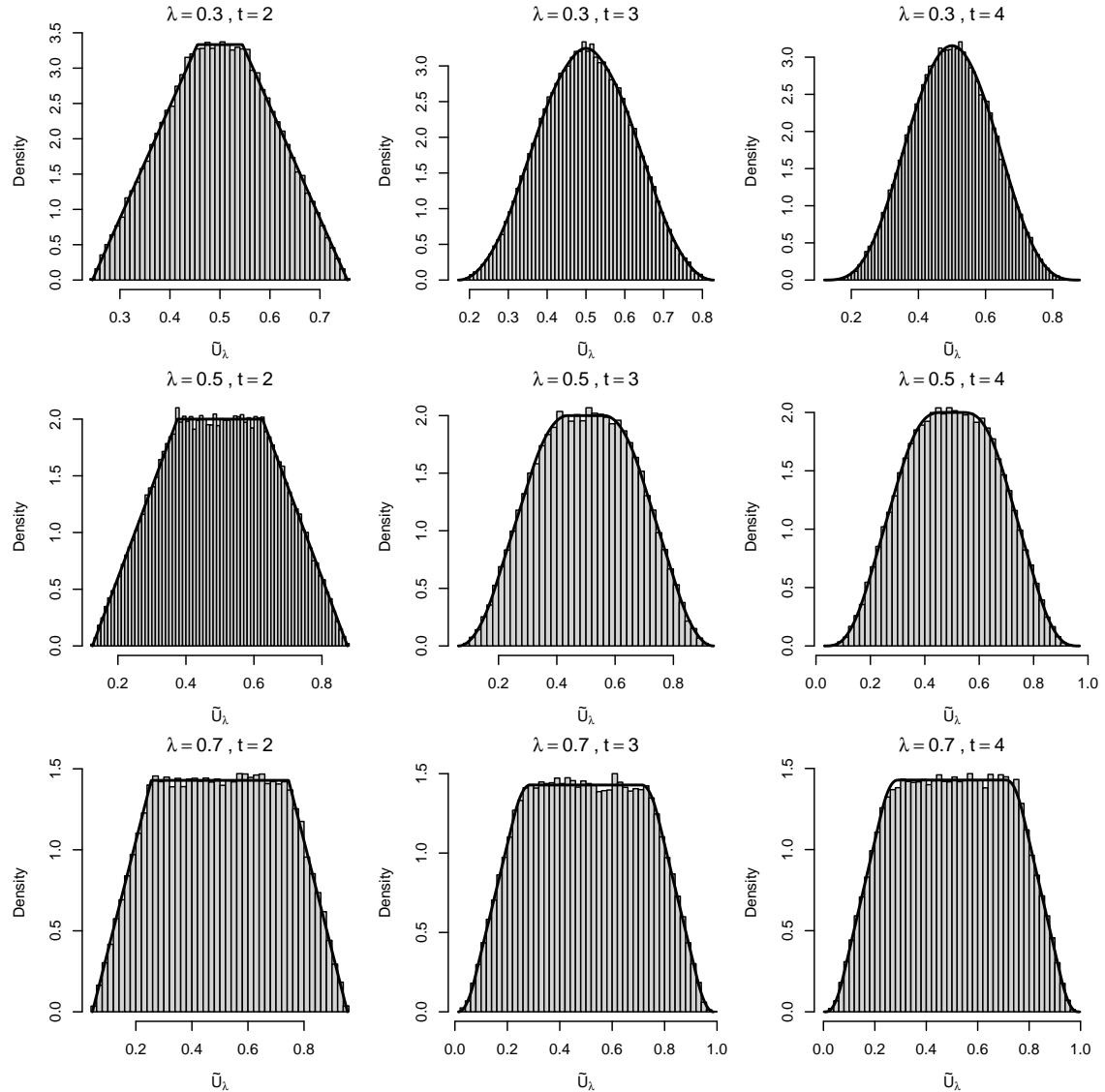


Figure 1: Plots of PDFs of the random variables  $\tilde{U}_{\lambda,t}$  with initialisation  $u_0 = 1/2$ , for  $\lambda \in \{0.3, 0.5, 0.7\}$  and  $t \in \{2, 3, 4\}$  along with histograms of 10000 replicates of the corresponding variable.

Table 7: Average run lengths  $R$ , numbers of detected OOC directions at time of alarm  $\#\text{OOC}$ , and numbers of single time point family wise errors (at time  $t = 1$ ) for  $d = 3$  variable normal model tested using the procedure from Section 3.1 with  $Z$ -tests. Average run lengths and number of true positives are reported via 100 simulation replications, while single time point family wise errors are obtained from 10000 simulations.

$\delta$	$\rho$	$\alpha$	Mean $R$	Mean $\#\text{OOC}$	Mean FWEs
0.5	0	0.01	53.72	0.81	0.0044
0.5	0	0.05	13.55	0.78	0.0230
0.5	0.5	0.01	70.98	0.87	0.0037
0.5	0.5	0.05	12.67	0.85	0.0201
0.5	0.9	0.01	66.05	0.99	0.0037
0.5	0.9	0.05	15.47	1.00	0.0245
1	0	0.01	15.38	0.99	0.0038
1	0	0.05	5.55	1.06	0.0198
1	0.5	0.01	17.7	0.96	0.0037
1	0.5	0.05	5.99	0.96	0.0220
1	0.9	0.01	14.8	1.00	0.0047
1	0.9	0.05	6.57	1.00	0.0259

only one, or neither) at the time of alarm. To address the FWER guarantee of Proposition 13, we conduct 10000 replicates of a one time point run (i.e.,  $t = 1$ ) and compute the average number of family-wise errors (FWEs) over those runs. The results of these simulations appear in Table 7.

In our second scenario, we consider instead that  $X_0 \sim \text{Cauchy}(\mu_0, \Sigma)$  is a  $d = 3$  dimensional random vector whose distribution is multivariate Cauchy with location parameter  $\mu_0 = 0$  and scale parameter  $\Sigma$  (see, e.g., Kotz & Nadarajah, 2004), where  $\Sigma$  is defined as above. At time  $t \in \mathbb{N}$ , we then consider  $X_t \sim \text{Cauchy}(\mu, \Sigma)$ , where  $\mu$  is the centroid parameter for the multivariate Cauchy and is defined as above. We will consider a two-phase design where in Phase I we observe an IID sample  $\mathbf{X}_0$  of size  $n_0 \in \{20, 50, 100\}$  and in Phase II, we observe an IID sample  $\mathbf{X}_t$  of size  $n_t = N_t \sim \text{DiscUnif}[n_0 - 10, n_0 + 10]$ . We wish to test the directional hypotheses at each time  $t$  that the median of the distribution at time  $t$  for each coordinate  $j \in [d]$  has experienced an upward or downward shift (i.e.,  $\mu_j - \mu_{0,j} > 0$  or  $\mu_j - \mu_{0,j} < 0$ ) from that of the Phase I process. To this end, we employ one-sided Mann–Whitney  $U$ -tests (see, e.g., Gibbons & Chakraborti, 2010, Sec. 5.7) to generate our sequences of  $p$ -values  $\left(P_t^{(j,\square)}\right)_t$ . We assess the performance of the procedure from Section 3.1 with these  $p$ -values, over the same configurations as above. To assess the power, 100 replications of simulation runs are used to compute the average  $R$  and  $\#\text{OOC}$  at the time of alarm. Simulation average FWEs are computed via 10000 replicates of a one time-point run (i.e.,  $t = 1$ ), and the results for  $n_0 = 50$  are reported in Table 8, with the results for  $n_0 = 20$  and 100 reported in Tables 14 and 15, respectively.

Table 8: Average run lengths  $R$ , numbers of detected OOC directions at time of alarm  $\#\text{OOC}$ , and numbers of single time point family wise errors (at time  $t = 1$ ) for  $d = 3$  variable Cauchy model with  $n_0 = 50$  tested using the procedure from Section 3.1 with Mann–Whitney  $U$ -tests. Average run lengths and number of true positives are reported via 100 simulation replications, while single time point family wise errors are obtained from 10000 simulations.

$\delta$	$\rho$	$\alpha$	Mean $R$	Mean $\#\text{OOC}$	Mean FWEs
0.5	0	0.01	224.49	0.92	0.0023
0.5	0	0.05	11.14	0.97	0.0195
0.5	0.5	0.01	71.7	0.98	0.004
0.5	0.5	0.05	9.7	1	0.0212
0.5	0.9	0.01	33.39	1	0.0036
0.5	0.9	0.05	6.21	0.99	0.0252
1	0	0.01	2.86	1.2	0.0044
1	0	0.05	1.76	1.47	0.0319
1	0.5	0.01	1.98	1.13	0.0053
1	0.5	0.05	1.13	1.36	0.0289
1	0.9	0.01	1.85	1.06	0.0054
1	0.9	0.05	1.04	1.3	0.0231

## 4.5 Results

In Tables 1 and 2, we observe that the IC bounds on the ARL and  $k$ -ARL from Propositions 1–4 are faithful albeit somewhat conservative. In particular, the ratio between the realised mean  $R_k$  and the corresponding lower bound can be as high as 23.89, although Table 2 also shows that in some non-trivial situations the bounds can be quite sharp, with ratios as low as 1.24 between the realised mean ARL and the lower bound. Furthermore, Table 2 shows that the bounds behave as predicted in both the (marginal) super-uniformity and conditional super-uniformity settings.

In Section 4.2, we demonstrate the construction of a nontrivial EWMA-like chart for KS tests under VSS, whose theoretical properties could not be analysed without the techniques from this work. From Table 3, we observe that the  $p$ -value charts without weighted averaging realise the bounds of Propositions 1 and 3. As with the results from Section 4.1, these bounds are realised somewhat conservatively, with ratios between the realised mean and the bound as high as 32.94 and as low as 6.51. We also observe that larger  $\alpha$  levels tend to decrease the discrepancy in the bound.

In Tables 4 and 9, we demonstrate that the EWMA-like  $p$ -value charts from Section 2.4.1 have correct lower bounds on the  $k$ -ARL. In particular, the  $k$ -ARL lower bounds can be extremely conservative, even in comparison to the non-averaged charts, with ratios as high as  $\approx 3500$  for some combinations of  $\lambda$  and  $r$ , although the ratio can be as low as 7.63. We further note that the charts with negative  $r$  tended to produce larger  $R_k$  values than those with positive  $r$ . We emphasise that we only tested a limited number of combinations of  $\lambda$  and  $r$ , exactly because for some choices, even at the modest  $\alpha$  levels assessed, the resulting  $R_k$  values can be arbitrarily large.

We note that although these charts can be conservative with respect to IC  $k$ -ARL control, they are nevertheless powerful across a range of OOC processes, as observed in Tables 5–11 and 6–13, where we assess performance under both the first alarm rule and the first  $k$  alarms rule for OOC detection.

From Tables 5, 10, and 11, we observe that in the persistent OOC setting the original  $p$ -value chart (without averaging) typically attains the smallest detection delays. Nevertheless, the penalty from averaging, a slightly larger time to detection in many scenarios, can be seen as a worthy trade in the face of the dramatic increases in the IC  $k$ -ARL levels that we observe.

The fact that the EWMA-like charts raise a first alarm no earlier than the  $p$ -value chart (i.e., the  $k = 1$  setting) at the same level  $\alpha$  comes down to the simple fact that for every  $r \neq 0$ ,  $\lambda \in (0, 1)$ , and  $t \geq 1$ ,

$$\tilde{Q}_{\lambda,t}^{(r)} \geq \min_{s \in [t]} P_s.$$

However, this type of ordering does not necessarily extend to the  $k$  alarms rule. Empirically, in the persistent OOC setting we still observe that the  $p$ -value chart raises an alarm before the EWMA-like charts in every tested scenario. The situation changes when considering the dynamic OOC settings in Tables 6, 12, and 13. Here we observe that in many cases it is possible for the EWMA-like charts with  $r < 0$  to raise, for example, a fifth alarm before the  $p$ -value chart does at the same  $\alpha$  level. This is quite atypical, since in most EWMA charts the extra power from moving averages is obtained by modifying the control limits, which require additional calibration and simulation to set (see, e.g., Lucas & Saccucci, 1990 and Reynolds & Stoumbos, 2005). Here, we observe that in the dynamic setting it is possible to gain additional power relative to the raw  $p$ -value chart under the  $k$  alarms rule, while simultaneously increasing the IC average time to the  $k$ th alarm, without any additional overhead of control-limit calibration.

The results from Figures 1 and 2 demonstrate directly the functional forms of the distributions arising from uniform EWMA charts, and verify the claims of Propositions 9 and 10. Lastly, Tables 7, 8, 14, and 15 provide evidence towards the correctness of Proposition 13 regarding the directional and coordinate localisation charts from Section 3.1. In all cases, we observe that the average FWE is controlled at the time of alarm, and is somewhat conservative as would be expected from the use of Bonferroni procedures. We also observe that at the time of alarm, usually only one direction (and typically only one coordinate) is identified at a time, and that power increases with the size of the OOC deviation and the degree of correlation between the coordinates. In addition, these results provide a demonstration of a viable localisation approach in the face of pathological Cauchy data with strong theoretical guarantees.

## 5 Concluding remarks

In this work, we have developed a general framework for SPC based on charting  $p$ -values. The key requirement underlying our IC guarantees is the super-uniformity property (1), which is satisfied by any valid  $p$ -value construction, irrespective of the underlying DGP and without any assumption on stochastic dependence. Within this framework, the simple Shewhart-type rule that raises an alarm whenever  $P_t \leq \alpha$  admits universal lower bounds on the ARL and its natural generalisation, the  $k$ -ARL. In particular, Propositions 1 and 3 provide worst-case IC guarantees under (1), and Propositions 2 and 4 show that these bounds improve to the familiar  $\alpha^{-1}$  and  $k\alpha^{-1}$  sharp rates when conditional super-uniformity (3) holds. Taken together, these results permit calibration of  $p$ -value charts in a manner that is valid for all DGPs for which  $H_0$  holds, and mitigate against the reliance on simulation-based ARL calibration tied to any parametric assumptions.

Further to these ARL results, we have demonstrated that  $p$ -values can support meaningful weighted averaging schemes, despite the fact that naive averaging of  $p$ -values generally fails to preserve validity. By leveraging recent results on merging functions for dependent  $p$ -values, we constructed EWMA-like schemes that produce, at each time  $t$ , a new  $p$ -value for the hypothesis that  $H_0$  holds for all time points up to time  $t$  (Propositions 6 and 7). This provides a generic route to constructing smoothed charts whose IC behaviour remains theoretically controlled, without the additional overhead of control-limit calibration. We also studied the distribution theory of uniform EWMA processes, both to clarify why naive uniform EWMA charts do not generally yield super-uniform tails, and to obtain explicit distributional formulae and left-tail guarantees (Propositions 9 and 10). Complementary constructions based on  $e$ -values and  $p$ -to- $e$  calibrators appear in the Appendix, providing additional flexibility in how one may design valid averaged charts.

We have further shown that the  $p$ -value framework extends naturally to the problem of directional and coordinate localisation in multivariate monitoring. Using a  $p$ -value-based closed-testing perspective and a Holm-type shortcut method, we obtained a procedure that can both raise a global alarm and then identify the set of affected coordinates and their corresponding OOC directions, while maintaining FWER control at level  $\alpha$  at the time of alarm. This yields a localisation approach that is modular in the choice of coordinate-wise test, and remains applicable in both one- and two-phase designs.

The examples and simulations in Section 4 illustrate several practical features of the methodology. First, the IC ARL and  $k$ -ARL lower bounds are faithful and, in some settings, sharp, while in others they can be conservative, which is the natural price of working without dependence assumptions. Second, the EWMA-like charts can trade additional IC conservativeness for OOC power across a range of alternatives, with particularly interesting behaviour under the  $k$ -alarms rule in dynamic OOC scenarios. Lastly, the localisation results provide a concrete demonstration that strong inferential guarantees remain attainable even in challenging multivariate settings, includ-

ing situations with heavy-tailed data. Within these constructions, we present two novel charts: an EWMA-like  $p$ -value chart based on KS statistics that can be used in two-phase designs for monitoring deviations from the IC distribution, and a nonparametric localisation chart, based on Mann–Whitney  $U$ -statistics for non-standard scenarios such as heavy-tailed settings.

There are a number of natural directions for further work. It would be useful to develop principled guidance for selecting the averaging parameters (such as  $\lambda$  and  $r$ ) to balance OOC detection and IC conservativeness, and to study whether alternative merging functions can reduce conservativeness while retaining the same level of robustness. On the multivariate side, it is of interest to investigate localisation procedures that exploit dependence structure to improve power while still providing FWER control at the time of alarm. More broadly, the  $p$ -value charting perspective suggests a modular approach to SPC: given any setting where one can construct valid  $p$ -values for  $H_0$ , one can immediately obtain charts with explicit IC guarantees, and layer on additional structure, including smoothing and localisation, without sacrificing theoretical control of ARL and  $k$ -ARL.

## Data availability statement

The data and code that support the findings of this study are openly available at [https://github.com/hiendn/Pvalue\\_SPC](https://github.com/hiendn/Pvalue_SPC).

## References

- Ahmed, F., Mahmood, T., Riaz, M., & Abbas, N. (2025). Comprehensive review of high-dimensional monitoring methods: trends, insights, and interconnections. *Quality Technology & Quantitative Management*, 22(4), 727–751.
- Albers, W. (2010). The optimal choice of negative binomial charts for monitoring high-quality processes. *Journal of Statistical Planning and Inference*, 140(1), 214–225.
- Albers, W. (2011). Control charts for health care monitoring under overdispersion. *Metrika*, 74(1), 67–83.
- Bakir, S. T. (2012). A nonparametric shewhart-type quality control chart for monitoring broad changes in a process distribution. *International Journal of Quality, Statistics, and Reliability*, 2012, 147520.
- Berger, R. L. & Boos, D. D. (1994).  $P$  values maximized over a confidence set for the nuisance parameter. *Journal of the American Statistical Association*, 89(427), 1012–1016.
- Chakraborti, S. & Graham, M. A. (2019). *Nonparametric Statistical Process Control*. John Wiley & Sons.

- Chen, P.-W. (2025). The statistical design of ccc-r chart with runs rules for a high-yield dependent process. *Journal of Statistical Computation and Simulation*. Published online 3 November 2025.
- Dickhaus, T. (2014). *Simultaneous Statistical Inference: With Applications in the Life Sciences*. Berlin, Heidelberg: Springer.
- Gibbons, J. D. & Chakraborti, S. (2010). *Nonparametric Statistical Inference*. Number 131 in Statistics: A Series of Textbooks and Monographs. Boca Raton, FL: Chapman and Hall/CRC, fifth edition.
- Grigg, O. A. & Spiegelhalter, D. J. (2008). An empirical approximation to the null unbounded steady-state distribution of the cumulative sum statistic. *Technometrics*, 50(4), 501–511.
- Grigg, O. A., Spiegelhalter, D. J., & Jones, H. E. (2009). Local and marginal control charts applied to methicillin resistant *Staphylococcus aureus* bacteraemia reports in uk acute national health service trusts. *Journal of the Royal Statistical Society: Series A (Statistics in Society)*, 172(1), 49–66.
- Gut, A. (2013). *Probability: A Graduate Course*. Springer Texts in Statistics. New York, NY: Springer, 2 edition.
- Hawkins, D. M. (1991). Multivariate quality control based on regression-adjusted variables. *Technometrics*, 33(1), 61–75.
- Heller, R. & Solari, A. (2024). Simultaneous directional inference. *Journal of the Royal Statistical Society: Series B (Statistical Methodology)*, 86(3), 650–670.
- Holm, S. (1979). A simple sequentially rejective multiple test procedure. *Scandinavian Journal of Statistics*, 6(2), 65–70.
- Joeckes, S., Smrek, M., & Righetti, A. F. (2016). A comparative study of two proposed CCC-r charts for high quality processes and their application to an injection molding process. *Quality Engineering*, 28(4), 467–475.
- Khrueasom, P. & Pongpullponsak, A. (2016). The integrated model of the kolmogorov–smirnov distribution-free statistic approach to process control and maintenance. *Journal of King Saud University – Science*, 29(2), 182–190.
- Knoth, S. (2005). Accurate ARL computation for EWMA- $s^2$  control charts. *Statistics and Computing*, 15(4), 341–352.
- Kotz, S. & Nadarajah, S. (2004). *Multivariate t-Distributions and Their Applications*. Cambridge Series in Statistical and Probabilistic Mathematics. Cambridge: Cambridge University Press.

- Lattimore, T. & Szepesvári, C. (2020). *Bandit Algorithms*. Cambridge, UK: Cambridge University Press.
- Lehmann, E. L. & Romano, J. P. (2005). Generalizations of the familywise error rate. *Annals of Statistics*, 33(3), 1138–1154.
- Lehmann, E. L. & Romano, J. P. (2022). *Testing Statistical Hypotheses*. Springer, 4 edition.
- Li, Y. & Tsung, F. (2009). False discovery rate-adjusted charting schemes for multistage process monitoring and fault identification. *Technometrics*, 51(2), 186–205.
- Li, Z., Qiu, P., Chatterjee, S., & Wang, Z. (2013). Using p values to design statistical process control charts. *Statistical Papers*, 54(2), 523–539.
- Lowry, C. A., Woodall, W. H., Champ, C. W., & Rigdon, S. E. (1992). A multivariate exponentially weighted moving average control chart. *Technometrics*, 34(1), 46–53. MEWMA; exact  $\chi^2_p$  reference when  $\Sigma$  known.
- Lu, C.-W. & Reynolds, M. R., J. (1999). EWMA control charts for monitoring the mean of autocorrelated processes. *Journal of Quality Technology*, 31, 166–188. EWMA design under autocorrelation.
- Lucas, J. M. & Saccucci, M. S. (1990). Exponentially weighted moving average control schemes: Properties and enhancements. *Technometrics*, 32(1), 1–12.
- Marcus, R., Peritz, E., & Gabriel, K. R. (1976). On closed testing procedures with special reference to ordered analysis of variance. *Biometrika*, 63(3), 655–660.
- Mason, R. L., Tracy, N. D., & Young, J. C. (1995). Decomposition of  $t^2$  for multivariate control chart interpretation. *Journal of Quality Technology*, 27(2), 99–108.
- Nikiforov, A. M. (1994). Algorithm as 288: Exact smirnov two-sample tests for arbitrary distributions. *Journal of the Royal Statistical Society Series C: Applied Statistics*, 43(1), 265–270.
- Ohta, H., Kusukawa, E., & Rahim, A. (2001). A CCC-r chart for high-yield processes. *Quality and Reliability Engineering International*, 17(6), 439–446.
- Page, E. S. (1954). Continuous inspection schemes. *Biometrika*, 41(1/2), 100–115.
- Qiu, P. (2013). *Introduction to Statistical Process Control*. Chapman and Hall/CRC.
- Reynolds, Marion R., J. & Stoumbos, Z. G. (2005). Should exponentially weighted moving average and cumulative sum charts be used with Shewhart limits? *Technometrics*, 47(4), 409–424.

- Roberts, S. W. (1959). Control chart tests based on geometric moving averages. *Technometrics*, 1(3), 239–250.
- Ross, G. J. (2015). Parametric and nonparametric sequential change detection in R: The cpm package. *Journal of Statistical Software*, 66(3), 1–20.
- Ross, G. J. & Adams, N. M. (2012). Two nonparametric control charts for detecting arbitrary distribution changes. *Journal of Quality Technology*, 44(2), 102–116.
- Shewhart, W. A. (1931). *Economic Control of Quality of Manufactured Product*. D. Van Nostrand Company.
- Tan, M. H. Y. & Shi, J. (2012). A bayesian approach for interpreting mean shifts in multivariate quality control. *Technometrics*, 54(3), 294–307.
- Tsung, F., Wang, K., Shang, Y., & Ning, M. (2025). Statistical process control: Recent advances. In M. Lovrić (Ed.), *International Encyclopedia of Statistical Science* (pp. 2564–2569). Springer.
- Vovk, V., Wang, B., & Wang, R. (2022). Admissible ways of merging p-values under arbitrary dependence. *The Annals of Statistics*, 50(1), 351–375.
- Vovk, V. & Wang, R. (2020). Combining p-values via averaging. *Biometrika*, 107(4), 791–808.
- Vovk, V. & Wang, R. (2021). E-values: Calibration, combination, and applications. *The Annals of Statistics*, 49(3), 1736–1754.
- Waqas, M., Xu, S. H., Hussain, S., & Aslam, M. U. (2024). Control charts in healthcare quality monitoring: a systematic review and bibliometric analysis. *International Journal for Quality in Health Care*, 36(3), mzae060.
- Xie, M., Goh, T. N., & Kuralmani, V. (2002). *Statistical Models and Control Charts for High-Quality Processes*. Springer.
- Xie, M., Goh, T. N., & Lu, X. S. (1998). Computer-aided statistical monitoring of automated manufacturing processes. *Computers & Industrial Engineering*, 35(1–2), 189–192.
- Xiong, D. & Xu, F. (2025). A robust diagnostic approach in mean shifts for multivariate statistical process control. *Journal of Statistical Computation and Simulation*, 95(3), 507–524. First published online 30 Nov 2024.
- Xu, F. & Deng, X. (2023). Joint diagnosis of process mean vector and covariance matrix for multivariate statistical process control. *Computers & Industrial Engineering*, 179, 109222.
- Xu, F., Shu, L., Li, Y., & Wang, B. (2023). Joint diagnosis of high-dimensional process mean and covariance matrix based on bayesian model selection. *Technometrics*, 65(4), 465–479.

Yeh, A. B., Lin, D. K. J., Zhou, H., & Venkataramani, C. (2003). A multivariate exponentially weighted moving average control chart for monitoring process variability. *Journal of Applied Statistics*, 30(5), 507–536.

Zwetsloot, I. M. & Woodall, W. H. (2021). A review of some sampling and aggregation strategies for basic statistical process monitoring. *Journal of Quality Technology*, 53(1), 1–16.

## Appendix

### EWMA charts based on $e$ -values

We say that a random variable  $E : \Omega \rightarrow [0, \infty]$  is an  $e$ -value with respect to the probability measure  $P_0$  if  $E_0 [E] \leq 1$ . Further, a function  $\gamma : [0, 1] \rightarrow \mathbb{R}_{\geq 0} \cup \{\infty\}$  is a  $p$ -to- $e$  calibrator if, for each  $p$ -value  $P$  satisfying  $P_0 (P \leq \alpha) \leq \alpha$  for every  $\alpha \in [0, 1]$ , it holds that  $E_0 [\gamma (P)] \leq 1$ . The following result appears as Proposition 2.1 of Vovk & Wang (2021).

**Lemma 14.** *A decreasing function  $\gamma : [0, 1] \rightarrow \mathbb{R}_{\geq 0} \cup \{\infty\}$  is a  $p$ -to- $e$  calibrator if and only if  $\int_0^1 \gamma (p) dp \leq 1$ .*

We now leverage Lemma 14 to obtain EWMA-like charts. To do so, we first note that given a set of  $e$ -values  $E_1, \dots, E_m : \Omega \rightarrow [0, \infty]$ , it holds that any convex combination of these  $e$ -values remains an  $e$ -value. That is, for any set of weights  $w_1, \dots, w_m \in [0, 1]$  such that  $\sum_{t=1}^m w_t = 1$ , the inequality

$$E_0 \left[ \sum_{t=1}^m w_t E_t \right] = \sum_{t=1}^m w_t E_0 [E_t] \leq \sum_{t=1}^m w_t = 1,$$

holds regardless of what the dependence behaviour between the  $e$ -values is. Another simple fact is that, given an  $e$ -value  $E$ , the random variable  $P = \min \{1, 1/E\}$  is a  $p$ -value, since Markov's inequality implies that, for  $\alpha \in (0, 1]$ ,

$$P_0 (P \leq \alpha) = P_0 (1/E \leq \alpha) = P_0 \left( E \geq \frac{1}{\alpha} \right) \leq \alpha E_0 [E] \leq \alpha.$$

Putting these two pieces together, to generate a sequence of  $p$ -values that averages information across the history, we first convert the  $p$ -values  $(P_t)_t$  into corresponding  $e$ -values  $(E_t)_t$ , defined by  $E_t = \gamma (P_t)$ , where  $\gamma$  satisfies the conditions of Lemma 14. Then, we generate an EWMA sequence  $(\tilde{E}_{\lambda,t})_t$  using these  $e$ -values by computing

$$\tilde{E}_{\lambda,t} = \lambda E_t + (1 - \lambda) \tilde{E}_{\lambda,t-1},$$

for  $t \geq 2$ , where  $\tilde{E}_{\lambda,1} = E_1$  and  $\lambda \in (0, 1)$ . We then obtain a super-uniform sequence of  $p$ -values with time-averaged information  $(Q_{\lambda,t}^e)_t$ , defined by

$$Q_{\lambda,t}^e = \min \left\{ 1, 1/\tilde{E}_{\lambda,t} \right\}.$$

**Proposition 15.** *For each  $\lambda \in (0, 1)$ , if  $(P_t)_t$  satisfies (1), then  $(Q_{\lambda,t}^e)_t$  is a super-uniform sequence under  $P_0$ ; i.e., for each  $\alpha \in [0, 1]$ ,*

$$P_0(Q_{\lambda,t}^e \leq \alpha) \leq \alpha \quad \text{for all } t \in \mathbb{N}.$$

We note that there are many choices for the  $p$ -to- $e$  calibrator  $\gamma$ , and  $P = \min\{1, 1/E\}$  is not the only method for generating a  $p$ -value from an  $e$ -value. However, the choice  $P = \min\{1, 1/E\}$  is admissible in the sense that it is pointwise no larger than every other transformation of  $E$  that yields a super-uniform  $p$ -value. On the other hand, there is no best choice for  $\gamma$ , although it is known that  $\gamma$  is admissible in the sense that there is no other calibrator that yields a valid  $e$ -value and is pointwise larger than  $\gamma(p)$ , if and only if  $\lim_{p \rightarrow 0} \gamma(p) = \infty$  and  $\int_0^1 \gamma(p) dp = 1$ . Thus, our suggested calibrator  $\gamma(p) = \beta p^{\beta-1}$ , for  $\beta \in (0, 1)$ , is an admissible and simple choice. These optimality results can be obtained from Vovk & Wang (2021, Sec. 2).

Lastly, we do not know of a useful method for producing time-averaged  $p$ -values using the  $e$ -value approach that yields a sequence of conditionally super-uniform  $p$ -values from an initial sequence  $(P_t)_t$  satisfying (3).

## Proofs of technical results

### Proof of Proposition 1

Let  $\nu = \lfloor 1/\alpha \rfloor$ . Then  $1 - (m-1)\alpha > 0$ , for  $m \in [\nu]$  and  $1 - \nu\alpha \geq 0$  at  $m = \nu + 1$ . Thus,

$$\sum_{m=1}^{\infty} [1 - (m-1)\alpha]_+ = \sum_{m=1}^{\nu+1} (1 - (m-1)\alpha) = (\nu+1) \left( 1 - \frac{\alpha\nu}{2} \right).$$

Next, write  $u = 1/\alpha$ . Then

$$(\nu+1) \left( 1 - \frac{\alpha\nu}{2} \right) = (\nu+1) \left( 1 - \frac{\nu}{2u} \right) = \frac{1}{2} \left\{ 2(\nu+1) - \frac{\nu(\nu+1)}{u} \right\}.$$

Observe that

$$2u(\nu+1) - \nu(\nu+1) \geq u^2 + u \text{ iff } (u - \nu)(u - (\nu+1)) \leq 0,$$

which holds for each  $\nu \leq u < \nu + 1$  (by the definition of  $\nu$ ). Therefore, from (2) we obtain the desired conclusion.

## Proof of Proposition 2

Let us write  $I_t = \mathbf{1}_{\{P_t \leq \alpha\}}$  and note that the run length can be written as  $R = \inf \{t \geq 1 : I_t = 1\}$ . Then, with

$$\mathbb{S}_t = \left\{ \sum_{s=1}^t I_s = 0 \right\} = \{I_1 = \dots = I_t = 0\},$$

we can write  $\{R > t\} = \mathbb{S}_t$ .

Since  $I_t : \Omega \rightarrow \{0, 1\}$ , (3) gives  $E_0(I_t | \mathcal{F}_{t-1}) \leq \alpha$ , and hence

$$P_0(I_t = 0 | \mathcal{F}_{t-1}) = E_0(1 - I_t | \mathcal{F}_{t-1}) \geq 1 - \alpha, \text{ a.s.}$$

Thus, by the tower property and since  $\mathbb{S}_{t-1} \in \mathcal{F}_{t-1}$ ,

$$\begin{aligned} P_0(\mathbb{S}_t) &= E_0 \mathbf{1}_{\mathbb{S}_t} = E_0 [\mathbf{1}_{\mathbb{S}_{t-1}} (1 - I_t)] \\ &= E_0 [\mathbf{1}_{\mathbb{S}_{t-1}} E_0 (1 - I_t | \mathcal{F}_{t-1})] \\ &\geq (1 - \alpha) E_0 \mathbf{1}_{\mathbb{S}_{t-1}} = (1 - \alpha) P_0(\mathbb{S}_{t-1}). \end{aligned}$$

Iterated applications of this bound then yield

$$P_0(R > t) = P_0(\mathbb{S}_t) \geq (1 - \alpha)^t,$$

noting that  $P_0(\mathbb{S}_0) = 1$ . The survival function expression for the expectation formula then gives

$$E_0 R = \sum_{t=0}^{\infty} P_0(R > t) \geq \sum_{t=0}^{\infty} (1 - \alpha)^t = \frac{1}{\alpha},$$

as required, by geometric summation.

## Proof of Proposition 3

For any  $m \geq 1$ , by Markov's inequality,

$$P_0(R_k \leq m) = P_0 \left( \sum_{t=1}^m \mathbf{1}_{\{P_t \leq \alpha\}} \geq k \right) \leq \frac{\sum_{t=1}^m E_0 \mathbf{1}_{\{P_t \leq \alpha\}}}{k} \leq \frac{\alpha m}{k}.$$

Thus  $P_0(R_k \geq m+1) \geq 1 - \alpha m/k$ . Using the survival function representation for the expectation,  $E_0 R_k = \sum_{m=0}^{\infty} P_0(R_k \geq m+1)$ , we obtain

$$E_0 R_k \geq \sum_{m=0}^{\nu} \left( 1 - \frac{\alpha m}{k} \right) = (\nu + 1) \left( 1 - \frac{\alpha \nu}{2k} \right),$$

upon discarding the negative terms. The second inequality follows by an argument analogous to the proof of Proposition 1.

### Proof of Proposition 4

Recall the notation  $I_t = \mathbf{1}_{\{P_t \leq \alpha\}}$  and define  $M_t = \sum_{s=1}^t (I_s - \alpha)$ ,  $N_t = \sum_{s=1}^t I_s = M_t + \alpha t$ , and  $M_0 = 0$ . Since  $\mathbb{E}_0 [I_t | \mathcal{F}_{t-1}] \leq \alpha$ , we have  $\mathbb{E}_0 [M_t | \mathcal{F}_{t-1}] \leq M_{t-1}$ , so  $(M_t)_t$  is a supermartingale adapted to  $(\mathcal{F}_t)_t$ .

Let  $T_m = \min \{R_k, m\}$  be a bounded stopping time. Note that

$$R_k = \inf \{t \geq 1 : N_t \geq k\},$$

and, because  $N_t$  increases by at most one at each step,  $N_{R_k} = k$  on  $\{R_k < \infty\}$ . By Doob's optional stopping theorem for bounded stopping times (see, e.g., Lattimore & Szepesvári, 2020, Thm. 3.8),  $\mathbb{E}_0 M_{T_m} \leq \mathbb{E}_0 M_0 = 0$ , implying

$$\mathbb{E}_0 N_{T_m} \leq \alpha \mathbb{E}_0 T_m. \quad (11)$$

Since  $T_m \nearrow R_k$  and  $T_m \geq 0$ , the monotone convergence theorem yields  $\lim_{m \rightarrow \infty} \mathbb{E}_0 T_m = \mathbb{E}_0 R_k$ . For the left-hand side,  $N_{T_m} \nearrow N_{R_k}$  almost surely; hence

$$\lim_{m \rightarrow \infty} \mathbb{E}_0 N_{T_m} = \mathbb{E}_0 N_{R_k} = k \mathbb{P}_0 (R_k < \infty) + \mathbb{E}_0 \left[ \lim_{t \rightarrow \infty} N_t \mathbf{1}_{\{R_k = \infty\}} \right] \leq k,$$

since on  $\{R_k = \infty\}$  we have  $\lim_{t \rightarrow \infty} N_t \leq k - 1$ . If  $\mathbb{P}_0 (R_k = \infty) > 0$ , then  $\mathbb{E}_0 R_k = \infty$  and the desired bound  $\mathbb{E}_0 R_k \geq k/\alpha$  is trivial. Otherwise,  $\mathbb{P}_0 (R_k < \infty) = 1$  and  $\lim_{m \rightarrow \infty} \mathbb{E}_0 N_{T_m} = k$ . Taking limits in (11) gives  $k \leq \alpha \mathbb{E}_0 R_k$ , as required.

### Proof of Proposition 6

Fix  $\lambda \in (0, 1)$ ,  $r > -1$  with  $r \neq 0$  and  $t \in \mathbb{N}$ . By (4) we can write

$$S_{\lambda,t}^{(r)} = \sum_{s=1}^t w_{t,s} P_s^r,$$

where the nonnegative weights  $w_{t,1}, \dots, w_{t,t}$  sum to 1 and have maximum  $w_{t,\max} = \max\{(1 - \lambda)^{t-1}, \lambda\}$ . The super-uniformity condition (1) implies that  $P_1, \dots, P_t$  are all  $p$ -values under  $\mathbb{P}_0$ .

If  $r \geq 1$ , then by Lemma 5(2), applied to  $P_1, \dots, P_t$  with weights  $w_{t,1}, \dots, w_{t,t}$ ,

$$q_t = \left( \min\{1 + r, w_{t,\max}^{-1}\} \right)^{1/r} \left( \sum_{s=1}^t w_{t,s} P_s^r \right)^{1/r} = Q_{\lambda,t}^{(r)}$$

is a valid  $p$ -value under  $P_0$ . If  $r \in (-1, 1) \setminus \{0\}$ , then Lemma 5(1) yields

$$q_t = (1+r)^{1/r} \left( \sum_{s=1}^t w_{t,s} P_s^r \right)^{1/r} = Q_{\lambda,t}^{(r)},$$

which is again a valid  $p$ -value under  $P_0$ . Therefore, in either case

$$P_0 \left( Q_{\lambda,t}^{(r)} \leq \alpha \right) = P_0 (q_t \leq \alpha) \leq \alpha$$

for every  $\alpha \in [0, 1]$ . Since  $t$  was arbitrary, the result follows.

### Proof of Proposition 7

Fix  $\lambda \in (0, 1)$ ,  $r \geq 1$  and  $t \geq 1$ . By construction,  $S_{\lambda,t-1}^{(r)}$  is a measurable function of  $(P_1, \dots, P_{t-1})$ , hence  $(1-\lambda) S_{\lambda,t-1}^{(r)}$  is  $\mathcal{F}_{t-1}$ -measurable and nonnegative. Therefore

$$\bar{Q}_{\lambda,t}^{(r)} = \lambda^{-1/r} \left\{ \lambda P_t^r + (1-\lambda) S_{\lambda,t-1}^{(r)} \right\}^{1/r} \geq \lambda^{-1/r} (\lambda P_t^r)^{1/r} = P_t,$$

so that

$$\left\{ \bar{Q}_{\lambda,t}^{(r)} \leq \alpha \right\} \subseteq \{P_t \leq \alpha\}, \text{ a.s.}$$

Taking conditional probabilities given  $\mathcal{F}_{t-1}$  and using (3) yields

$$P_0 \left( \bar{Q}_{\lambda,t}^{(r)} \leq \alpha \mid \mathcal{F}_{t-1} \right) \leq P_0 (P_t \leq \alpha \mid \mathcal{F}_{t-1}) \leq \alpha, \text{ a.s.},$$

which proves the claim.

### Proof of Proposition 9

To obtain the probability density function (PDF) of  $\tilde{U}_{\lambda,t}$ , observe that for each  $t \geq 1$ , with  $a_{t,s} = \lambda(1-\lambda)^{t-s}$ , we can write

$$\tilde{U}_{\lambda,t} = (1-\lambda)^t u_0 + \sum_{s=1}^t a_{t,s} U_s.$$

Thus,  $\tilde{U}_{\lambda,t} = (1-\lambda)^t u_0 + W_t$ , where  $W_t = \sum_{s=1}^t a_{t,s} U_s$  and  $U_s \sim \text{Unif}(0, 1)$  are IID, so that  $a_{t,s} U_s \sim \text{Unif}(0, a_{t,s})$ . Let

$$F_{t,u_0}(u) = P_0 \left( \tilde{U}_{\lambda,t} \leq u \right) = P_0 (W_t \leq u - (1-\lambda)^t u_0)$$

be the CDF of  $\tilde{U}_{\lambda,t}$ , and note that  $F_{t,u_0}(u) = G_t(u - (1-\lambda)^t u_0)$ , where  $G_t$  is the CDF of  $W_t$ . We write the respective PDFs of  $\tilde{U}_{\lambda,t}$  and  $W_t$  as  $f_{t,u_0}$  and  $g_t$ , respectively, and note that  $f_{t,u_0}(u) =$

$$g_t(u - (1 - \lambda)^t u_0).$$

For  $t = 1$ , observe that  $W_1 = a_{t,1}U_1 \sim \text{Unif}(0, a_{t,1})$ , thus

$$g_1(w) = \frac{1}{a_{t,1}} \mathbf{1}_{[0, a_{t,1}]}(w), \text{ and } G_1(w) = \frac{[w]_+ - [w - a_{t,1}]_+}{a_{t,1}}.$$

When  $t \geq 2$ , define  $\tilde{W}_t = a_{t,t}U_t \sim \text{Unif}(0, a_{t,t})$ , independent of  $W_{t-1}^{(t)} = \sum_{s=1}^{t-1} a_{t,s}U_s$ . Then

$$W_t = W_{t-1}^{(t)} + \tilde{W}_t,$$

and the convolution identity for the PDF of sums of independent random variables yields

$$g_t(w) = \int_{\mathbb{R}} g_{t-1}^{(t)}(w - \tilde{w}) h_t(\tilde{w}) d\tilde{w},$$

where  $h_t(\tilde{w}) = a_{t,t}^{-1} \mathbf{1}_{[0, a_{t,t}]}(\tilde{w})$  is the PDF of  $\tilde{W}_t$  and  $g_{t-1}^{(t)}$  denotes the PDF of  $W_{t-1}^{(t)}$ . Hence

$$g_t(w) = \frac{1}{a_{t,t}} \int_0^{a_{t,t}} g_{t-1}^{(t)}(w - \tilde{w}) d\tilde{w}. \quad (12)$$

We need the following lemma.

**Lemma 16.** *For each  $m \in \mathbb{N}$ ,  $a > 0$ , and  $x \in \mathbb{R}$ ,*

$$\int_0^a [x - y]_+^{m-1} dy = \frac{[x]_+^m - [x - a]_+^m}{m}.$$

*Proof.* If  $x \leq 0$ , then both sides are equal to zero. If  $0 < x < a$ , then

$$\int_0^a [x - y]_+^{m-1} dy = \int_0^x (x - y)^{m-1} dy = \left[ -\frac{(x - y)^m}{m} \right]_{y=0}^{y=x} = \frac{x^m}{m}.$$

Finally, if  $x \geq a$ , then

$$\int_0^a [x - y]_+^{m-1} dy = \int_0^a (x - y)^{m-1} dy = \left[ -\frac{(x - y)^m}{m} \right]_{y=0}^{y=a} = \frac{x^m - (x - a)^m}{m}.$$

The result follows by combining the cases.  $\square$

We proceed by induction on  $t$ . The case  $t = 1$  has been verified. For  $t - 1 \geq 1$ , make the inductive hypothesis

$$g_{t-1}^{(t)}(w) = \frac{1}{(t-2)! \prod_{s=1}^{t-1} a_{t,s}} \sum_{\mathbb{S} \subseteq [t-1]} (-1)^{|\mathbb{S}|} [w - a_{\mathbb{S}}]_+^{t-2},$$

where  $a_{\mathbb{S}} = \sum_{s \in \mathbb{S}} a_{t,s}$ . Then (12) and Lemma 16 give

$$\begin{aligned}
g_t(w) &= \frac{1}{a_{t,t}} \int_0^{a_{t,t}} \frac{1}{(t-2)! \prod_{s=1}^{t-1} a_{t,s}} \sum_{\mathbb{S} \subseteq [t-1]} (-1)^{|\mathbb{S}|} [w - \tilde{w} - a_{\mathbb{S}}]_+^{t-2} d\tilde{w} \\
&= \frac{1}{(t-1)! \prod_{s=1}^t a_{t,s}} \sum_{\mathbb{S} \subseteq [t-1]} (-1)^{|\mathbb{S}|} ([w - a_{\mathbb{S}}]_+^{t-1} - [w - a_{\mathbb{S}} - a_{t,t}]_+^{t-1}) \\
&= \frac{1}{(t-1)! \prod_{s=1}^t a_{t,s}} \sum_{\mathbb{S} \subseteq [t]} (-1)^{|\mathbb{S}|} [w - a_{\mathbb{S}}]_+^{t-1}.
\end{aligned}$$

Therefore,

$$\begin{aligned}
f_{t,u_0}(u) &= g_t(u - (1-\lambda)^t u_0) \\
&= \frac{1}{(t-1)! \prod_{s=1}^t a_{t,s}} \sum_{\mathbb{S} \subseteq [t]} (-1)^{|\mathbb{S}|} [u - (1-\lambda)^t u_0 - a_{\mathbb{S}}]_+^{t-1},
\end{aligned}$$

as claimed. Finally, for any  $a \in \mathbb{R}$  and  $m \geq 1$ ,  $(d/du) [u - a]_+^m = m [u - a]_+^{m-1}$ , so the fundamental theorem of calculus yields

$$\int_{-\infty}^u [x - a]_+^{t-1} dx = \frac{[u - a]_+^t}{t}.$$

Applying this identity termwise to  $f_{t,u_0}$  gives the CDF

$$F_{t,u_0}(u) = \frac{1}{t! \prod_{s=1}^t a_{t,s}} \sum_{\mathbb{S} \subseteq [t]} (-1)^{|\mathbb{S}|} [u - (1-\lambda)^t u_0 - a_{\mathbb{S}}]_+^t,$$

which completes the proof.

## Proof of Proposition 10

Recall that, with  $a_{t,s} = \lambda(1-\lambda)^{t-s}$ ,

$$\tilde{U}_{\lambda,t} = (1-\lambda)^t u_0 + \sum_{s=1}^t a_{t,s} U_s.$$

Define the centred sum  $\tilde{U}_{\lambda,t}^{\text{cent}} = \sum_{s=1}^t \{a_{t,s} U_s - a_{t,s}/2\}$  and  $c_t(u_0) = 1/2 + (1-\lambda)^t (u_0 - 1/2)$ , so that

$$\tilde{U}_{\lambda,t} = c_t(u_0) + \tilde{U}_{\lambda,t}^{\text{cent}}.$$

Since each  $a_{t,s} U_s - a_{t,s}/2 \sim \text{Unif}(-a_{t,s}/2, a_{t,s}/2)$ ,

$$\text{supp}(\tilde{U}_{\lambda,t}^{\text{cent}}) = [-\{1 - (1-\lambda)^t\}/2, \{1 - (1-\lambda)^t\}/2],$$

$$\text{supp}(\tilde{U}_{\lambda,t}) = [(1-\lambda)^t u_0, 1 - (1-\lambda)^t(1-u_0)].$$

For each  $t \in \mathbb{N}$ , let  $f_t^{\text{cent}}$  denote the PDF of  $\tilde{U}_{\lambda,t}^{\text{cent}}$ . To establish that  $f_t^{\text{cent}}$  is even and nonincreasing on  $[0, \infty)$ , fix  $t$  and define the partial centred sums, with the fixed weights  $a_{t,1}, \dots, a_{t,t}$ ,

$$\tilde{U}_{\lambda,t,m}^{\text{cent}} = \sum_{s=1}^m \{a_{t,s} U_s - a_{t,s}/2\}, \quad m = 1, \dots, t,$$

so that  $\tilde{U}_{\lambda,t,t}^{\text{cent}} = \tilde{U}_{\lambda,t}^{\text{cent}}$ . Let  $f_{t,m}^{\text{cent}}$  denote the PDF of  $\tilde{U}_{\lambda,t,m}^{\text{cent}}$ . For  $m = 1$ ,  $f_{t,1}^{\text{cent}} = 1/a_{t,1}$  on  $\text{supp}(\tilde{U}_{\lambda,t,1}^{\text{cent}}) = [-a_{t,1}/2, a_{t,1}/2]$ . More generally,  $\tilde{U}_{\lambda,t,m}^{\text{cent}} = \tilde{U}_{\lambda,t,m-1}^{\text{cent}} + V_{t,m}$ , where  $V_{t,m} \sim \text{Unif}(-a_{t,m}/2, a_{t,m}/2)$  is independent of  $\tilde{U}_{\lambda,t,m-1}^{\text{cent}}$ . The convolution identity gives

$$f_{t,m}^{\text{cent}}(u) = \frac{1}{a_{t,m}} \int_{-a_{t,m}/2}^{a_{t,m}/2} f_{t,m-1}^{\text{cent}}(u-v) \, dv.$$

Differentiating under the integral (Leibniz' rule) yields

$$\frac{d}{du} f_{t,m}^{\text{cent}}(u) = \frac{1}{a_{t,m}} \left( f_{t,m-1}^{\text{cent}}(u + a_{t,m}/2) - f_{t,m-1}^{\text{cent}}(u - a_{t,m}/2) \right).$$

If  $f_{t,m-1}^{\text{cent}}$  is nonincreasing on  $[0, \infty)$  and even, then  $f_{t,m}^{\text{cent}}$  is nonincreasing on  $[0, \infty)$ : i.e., when  $u \geq a_{t,m}/2$ ,  $u \pm a_{t,m}/2 \geq 0$  and nonincreasingness gives  $f_{t,m-1}^{\text{cent}}(u + a_{t,m}/2) \leq f_{t,m-1}^{\text{cent}}(u - a_{t,m}/2)$ ; when  $u \in [0, a_{t,m}/2]$ , evenness gives  $f_{t,m-1}^{\text{cent}}(u - a_{t,m}/2) = f_{t,m-1}^{\text{cent}}(a_{t,m}/2 - u)$  with  $a_{t,m}/2 - u \geq 0$ ; and then  $f_{t,m-1}^{\text{cent}}(u + a_{t,m}/2) \leq f_{t,m-1}^{\text{cent}}(a_{t,m}/2 - u) = f_{t,m-1}^{\text{cent}}(u - a_{t,m}/2)$ . Moreover, evenness is preserved under convolution with the symmetric uniform kernel, so  $f_{t,m}^{\text{cent}}$  is even whenever  $f_{t,m-1}^{\text{cent}}$  is even. Since  $f_{t,1}^{\text{cent}}$  is even and nonincreasing on  $[0, \infty)$ , induction implies that  $f_{t,t}^{\text{cent}}$  is even and nonincreasing on  $[0, \infty)$ . Since  $f_t^{\text{cent}}$  is the PDF of  $\tilde{U}_{\lambda,t}^{\text{cent}} = \tilde{U}_{\lambda,t,t}^{\text{cent}}$ , we conclude that  $f_t^{\text{cent}}$  is even and nonincreasing on  $[0, \infty)$ .

If  $g \geq 0$  is nonincreasing on  $[0, \bar{d}]$ , then for each  $d \in [0, \bar{d}]$ ,

$$\frac{1}{\bar{d}} \int_0^{\bar{d}} g(u) \, du \geq \frac{1}{\bar{d}} \int_0^{\bar{d}} g(u) \, du.$$

Applying this to  $g = f_t^{\text{cent}}$  with  $\bar{d} = \{1 - (1-\lambda)^t\}/2$  and using evenness, for each  $d \leq \{1 - (1-\lambda)^t\}/2$ ,

$$\int_0^d f_t^{\text{cent}}(u) \, du \geq \frac{d}{\bar{d}} \int_0^{\bar{d}} f_t^{\text{cent}}(u) \, du = \frac{2d}{1 - (1-\lambda)^t} \int_0^{\{1 - (1-\lambda)^t\}/2} f_t^{\text{cent}}(u) \, du = \frac{d}{1 - (1-\lambda)^t},$$

so

$$\text{P}_0(\tilde{U}_{\lambda,t}^{\text{cent}} \leq -d) = \frac{1}{2} - \int_0^d f_t^{\text{cent}}(u) \, du \leq \frac{1}{2} - \frac{d}{1 - (1-\lambda)^t}.$$

Fix  $\alpha \in [0, 1/2]$  and  $u_0 \geq 1/2$ , and set

$$d = c_t(u_0) - \alpha = (1/2 - \alpha) + (1 - \lambda)^t(u_0 - 1/2) \geq 0.$$

Then  $P_0(\tilde{U}_{\lambda,t} \leq \alpha) = P_0(\tilde{U}_{\lambda,t}^{\text{cent}} \leq -d)$ . If  $d > \{1 - (1 - \lambda)^t\}/2$ , the probability is  $0 \leq \alpha$  and we are done. Otherwise apply the bound above and use  $1 - (1 - \lambda)^t \leq 1$ :

$$P_0(\tilde{U}_{\lambda,t} \leq \alpha) \leq \frac{1}{2} - \frac{d}{1 - (1 - \lambda)^t} \leq \frac{1}{2} - d \leq \alpha,$$

as required.

### Proof of Proposition 13

We work with fixed time  $t$ . Recall that  $P_0$  be a probability measure under which the IC hypothesis  $H_0 : \theta = \theta_0$  holds at time  $t$ . Then, for every  $j \in [d]$  and  $\square \in \{\leq, \geq\}$ , the directional null  $H_0^{(j,\square)}$  is true, since  $\theta_j = \theta_{0,j}$  implies  $\theta_{0,j} \square \theta_j$ . Consequently,

$$\{\exists s \in \mathbb{D}_t : \theta_{0,j} \square \theta_j\} = \{\mathbb{D}_t \neq \emptyset\}.$$

By (10), for each  $j \in [d]$  the two-sided  $p$ -value  $P_t^j$  is super-uniform under the equality hypothesis  $H_0^j : \theta_j = \theta_{0,j}$ . Applying Holm's step-down procedure at level  $\alpha$  to  $\{P_t^j\}_{j \in [d]}$  produces the rejection set  $\mathbb{J}_t$ . By Theorems 11 and 12, Holm's procedure has strong FWER control at level  $\alpha$  for the family  $\{H_0^j\}_{j \in [d]}$ . Since  $H_0^j$  is true for every  $j \in [d]$  under  $P_0$ , we have

$$P_0(\mathbb{J}_t \neq \emptyset) \leq \alpha.$$

By the reporting rule in Section 3.1, the set  $\mathbb{D}_t$  is constructed from  $\mathbb{J}_t$  by assigning, for each  $j \in \mathbb{J}_t$ , exactly one direction  $\square \in \{\leq, \geq\}$ . In particular,  $\mathbb{D}_t \neq \emptyset$  implies  $\mathbb{J}_t \neq \emptyset$ , therefore,

$$P_0(\exists s \in \mathbb{D}_t : \theta_{0,j} \square \theta_j) \leq P_0(\mathbb{J}_t \neq \emptyset) \leq \alpha,$$

which is (9).

### Additional numerical results

We provide further numerical results from Section 4. Tables 9, 10, 11, 12 and 13 provide additional results for Section 4.2. Figure 2 provides additional visualisation for Section 4.3. Tables 14 and 15 provide additional results for Section 4.4.

Table 9: Average  $R_k$  while IC versus  $k$ -ARL bounds from Proposition 3 for KS EWMA-like  $p$ -value charts  $\left(\tilde{Q}_{\lambda,t}^{(r)}\right)_t$  and  $\left(\bar{Q}_{\lambda,t}^{(r)}\right)_t$ , using 100 simulation repetitions. This table contains results for  $n_0 \in \{100, 200\}$ , while Table 4 contains results for  $n_0 = 50$ .

Chart	$n_0$	$\alpha$	$k$	$\lambda$	$r$	mean $R_k$	st. err. $R_k$	lower bound	ratio
$\tilde{Q}_{\lambda,t}^{(r)}$	100	0.05	1	0.5	-0.9	36300.60	8129.78	10.5	3457.2000
	100	0.05	1	0.5	-0.8	17899.07	4642.61	10.5	1704.6733
	100	0.05	5	0.5	-0.9	170624.82	37579.01	50.5	3378.7093
	100	0.05	5	0.5	-0.8	83157.22	16025.42	50.5	1646.6776
	100	0.1	1	0.5	-0.9	15112.70	3629.50	5.5	2747.7636
	100	0.1	1	0.5	-0.8	4915.30	1010.26	5.5	893.6909
	100	0.1	5	0.5	-0.9	38756.87	6254.42	25.5	1520.8576
	100	0.1	5	0.5	-0.8	19485.31	3483.18	25.5	764.1298
	200	0.05	1	0.5	-0.9	36438.61	12501.96	10.5	3470.3438
	200	0.05	1	0.5	-0.8	13673.33	3899.34	10.5	1302.2229
	200	0.05	5	0.5	-0.9	163773.92	40044.39	50.5	3243.0489
	200	0.05	5	0.5	-0.8	61254.49	9087.68	50.5	1212.9602
	200	0.1	1	0.5	-0.9	12153.63	3262.65	5.5	2209.751
	200	0.1	1	0.5	-0.8	3806.43	658.28	5.5	692.0782
	200	0.1	5	0.5	-0.9	34633.98	5038.05	25.5	1358.1953
	200	0.1	5	0.5	-0.8	11625.17	2128.99	25.5	455.8882
$\bar{Q}_{\lambda,t}^{(r)}$	100	0.05	1	0.9	1	2358.38	632.10	10.5	224.6076
	100	0.05	1	0.95	1	584.18	110.88	10.5	55.6362
	100	0.05	5	0.9	1	7574.50	1252.08	50.5	149.9901
	100	0.05	5	0.95	1	2943.04	487.05	50.5	58.2770
	100	0.1	1	0.9	1	234.15	47.66	5.5	42.5727
	100	0.1	1	0.95	1	41.94	6.41	5.5	7.6255
	100	0.1	5	0.9	1	765.87	125.16	25.5	30.0330
	100	0.1	5	0.95	1	289.27	33.17	25.5	11.344
	200	0.05	1	0.9	1	2229.21	607.40	10.5	212.3057
	200	0.05	1	0.95	1	311.43	45.42	10.5	29.6590
	200	0.05	5	0.9	1	9698.15	2254.83	50.5	192.0426
	200	0.05	5	0.95	1	1703.18	230.54	50.5	33.7263
	200	0.1	1	0.9	1	105.28	20.25	5.5	19.1418
	200	0.1	1	0.95	1	49.17	8.48	5.5	8.9400
	200	0.1	5	0.9	1	785.69	108.18	25.5	30.8114
	200	0.1	5	0.95	1	218.23	24.79	25.5	8.5580

Table 10: Average  $R_k$  under persistent OOC processes for KS  $p$ -value charts  $(P_t)_t$ ,  $\left(\tilde{Q}_{\lambda,t}^{(r)}\right)_t$  and  $\left(\bar{Q}_{\lambda,t}^{(r)}\right)_t$ , using 100 simulation repetitions. This table contains results for  $n_0 = 100$ , while Appendix Tables 5 and 11 contains results for  $n_0 = 50$  and  $n_0 = 200$ , respectively.

OOC process	$n_0$	$\alpha$	Chart	$r$	$\lambda$	mean $R_1$	st. err. $R_1$	mean $R_5$	st. err. $R_5$	
N(1/2, 1)	100	0.01	$P_t$			2.27	0.57	10.28	1.23	
	100	0.01	$\tilde{Q}_{\lambda,t}^{(r)}$	-0.9	0.5	23.65	6.93	52.64	12.82	
	100	0.01	$\tilde{Q}_{\lambda,t}^{(r)}$	-0.8	0.5	13.49	6.07	56.24	28.13	
	100	0.01	$\tilde{Q}_{\lambda,t}^{(r)}$	1	0.9	9.46	4.16	49.26	27.41	
	100	0.01	$\bar{Q}_{\lambda,t}^{(r)}$	1	0.95	3.63	0.74	25.29	7.53	
	100	0.05	$P_t$			1.28	0.08	6.43	0.30	
	100	0.05	$\tilde{Q}_{\lambda,t}^{(r)}$	-0.9	0.5	6.71	2.11	28.66	8.20	
	100	0.05	$\tilde{Q}_{\lambda,t}^{(r)}$	-0.8	0.5	3.41	0.84	10.77	1.98	
	100	0.05	$\bar{Q}_{\lambda,t}^{(r)}$	1	0.9	1.56	0.13	11.81	3.24	
	100	0.05	$\bar{Q}_{\lambda,t}^{(r)}$	1	0.95	1.28	0.08	6.89	0.50	
	N(1, 1)	100	0.01	$P_t$		1.00	0.00	5.00	0.00	
		100	0.01	$\tilde{Q}_{\lambda,t}^{(r)}$	-0.9	0.5	1.00	0.00	5.00	0.00
		100	0.01	$\tilde{Q}_{\lambda,t}^{(r)}$	-0.8	0.5	1.01	0.01	5.01	0.01
		100	0.01	$\bar{Q}_{\lambda,t}^{(r)}$	1	0.9	1.00	0.00	5.00	0.00
		100	0.01	$\bar{Q}_{\lambda,t}^{(r)}$	1	0.95	1.00	0.00	5.00	0.00
		100	0.05	$P_t$		1.00	0.00	5.00	0.00	
		100	0.05	$\tilde{Q}_{\lambda,t}^{(r)}$	-0.9	0.5	1.00	0.00	5.00	0.00
		100	0.05	$\tilde{Q}_{\lambda,t}^{(r)}$	-0.8	0.5	1.00	0.00	5.00	0.00
		100	0.05	$\bar{Q}_{\lambda,t}^{(r)}$	1	0.9	1.00	0.00	5.00	0.00
		100	0.05	$\bar{Q}_{\lambda,t}^{(r)}$	1	0.95	1.00	0.00	5.00	0.00
N(0, 2)	100	0.01	$P_t$			73.99	15.95	328.15	52.35	
	100	0.01	$\tilde{Q}_{\lambda,t}^{(r)}$	-0.9	0.5	6354.41	1947.68	21834.59	6659.35	
	100	0.01	$\tilde{Q}_{\lambda,t}^{(r)}$	-0.8	0.5	2904.52	815.86	18591.21	4835.06	
	100	0.01	$\bar{Q}_{\lambda,t}^{(r)}$	1	0.9	12367.56	9731.56	49943.42	35538.48	
	100	0.01	$\bar{Q}_{\lambda,t}^{(r)}$	1	0.95	607.67	234.54	2346.59	477.43	
	100	0.05	$P_t$			9.25	1.43	43.07	4.30	
	100	0.05	$\tilde{Q}_{\lambda,t}^{(r)}$	-0.9	0.5	797.49	258.57	3114.35	731.10	
	100	0.05	$\tilde{Q}_{\lambda,t}^{(r)}$	-0.8	0.5	330.37	74.80	1389.18	274.72	
	100	0.05	$\bar{Q}_{\lambda,t}^{(r)}$	1	0.9	41.69	16.66	152.71	38.84	
	100	0.05	$\bar{Q}_{\lambda,t}^{(r)}$	1	0.95	11.66	1.93	59.13	7.83	
	Cauchy	100	0.01	$P_t$		15.72	1.88	82.13	7.66	
		100	0.01	$\tilde{Q}_{\lambda,t}^{(r)}$	-0.9	0.5	1272.56	305.43	3792.39	672.21
		100	0.01	$\tilde{Q}_{\lambda,t}^{(r)}$	-0.8	0.5	585.77	115.57	2275.66	384.01
		100	0.01	$\bar{Q}_{\lambda,t}^{(r)}$	1	0.9	147.44	37.90	698.28	205.49
		100	0.01	$\bar{Q}_{\lambda,t}^{(r)}$	1	0.95	53.31	9.13	238.25	30.51
		100	0.05	$P_t$		3.52	0.36	16.04	0.93	
		100	0.05	$\tilde{Q}_{\lambda,t}^{(r)}$	-0.9	0.5	119.95	16.23	532.01	92.31
		100	0.05	$\tilde{Q}_{\lambda,t}^{(r)}$	-0.8	0.5	96.66	26.42	294.28	51.08
		100	0.05	$\bar{Q}_{\lambda,t}^{(r)}$	1	0.9	4.05	0.49	20.80	1.76
		100	0.05	$\bar{Q}_{\lambda,t}^{(r)}$	1	0.95	3.44	0.37	17.55	1.43

Table 11: Average  $R_k$  under persistent OOC processes for KS  $p$ -value charts  $(P_t)_t$ ,  $\left(\tilde{Q}_{\lambda,t}^{(r)}\right)_t$  and  $\left(\bar{Q}_{\lambda,t}^{(r)}\right)_t$ , using 100 simulation repetitions. This table contains results for  $n_0 = 200$ , while Appendix Tables 5 and 10 contains results for  $n_0 = 50$  and  $n_0 = 100$ , respectively.

OOC process	$n_0$	$\alpha$	Chart	$r$	$\lambda$	mean $R_1$	st. err. $R_1$	mean $R_5$	st. err. $R_5$
N(1/2, 1)	200	0.01	$P_t$			1.04	0.02	5.22	0.07
	200	0.01	$\tilde{Q}_{\lambda,t}^{(r)}$	-0.9	0.5	1.68	0.34	7.36	1.61
	200	0.01	$\tilde{Q}_{\lambda,t}^{(r)}$	-0.8	0.5	1.28	0.09	5.44	0.13
	200	0.01	$\tilde{Q}_{\lambda,t}^{(r)}$	1	0.9	1.07	0.04	5.21	0.06
	200	0.01	$\bar{Q}_{\lambda,t}^{(r)}$	1	0.95	1.13	0.06	5.36	0.11
	200	0.05	$P_t$			1.00	0.00	5.01	0.01
	200	0.05	$\tilde{Q}_{\lambda,t}^{(r)}$	-0.9	0.5	1.22	0.07	5.25	0.08
	200	0.05	$\tilde{Q}_{\lambda,t}^{(r)}$	-0.8	0.5	1.03	0.02	5.06	0.03
	200	0.05	$\bar{Q}_{\lambda,t}^{(r)}$	1	0.9	1.00	0.00	5.06	0.03
	200	0.05	$\bar{Q}_{\lambda,t}^{(r)}$	1	0.95	1.01	0.01	5.06	0.02
N(1, 1)	200	0.01	$P_t$			1.00	0.00	5.00	0.00
	200	0.01	$\tilde{Q}_{\lambda,t}^{(r)}$	-0.9	0.5	1.00	0.00	5.00	0.00
	200	0.01	$\tilde{Q}_{\lambda,t}^{(r)}$	-0.8	0.5	1.00	0.00	5.00	0.00
	200	0.01	$\bar{Q}_{\lambda,t}^{(r)}$	1	0.9	1.00	0.00	5.00	0.00
	200	0.01	$\bar{Q}_{\lambda,t}^{(r)}$	1	0.95	1.00	0.00	5.00	0.00
	200	0.05	$P_t$			1.00	0.00	5.00	0.00
	200	0.05	$\tilde{Q}_{\lambda,t}^{(r)}$	-0.9	0.5	1.00	0.00	5.00	0.00
	200	0.05	$\tilde{Q}_{\lambda,t}^{(r)}$	-0.8	0.5	1.00	0.00	5.00	0.00
	200	0.05	$\bar{Q}_{\lambda,t}^{(r)}$	1	0.9	1.00	0.00	5.00	0.00
	200	0.05	$\bar{Q}_{\lambda,t}^{(r)}$	1	0.95	1.00	0.00	5.00	0.00
N(0, 2)	200	0.01	$P_t$			16.72	4.58	82.08	10.36
	200	0.01	$\tilde{Q}_{\lambda,t}^{(r)}$	-0.9	0.5	1045.80	316.58	2536.42	623.14
	200	0.01	$\tilde{Q}_{\lambda,t}^{(r)}$	-0.8	0.5	499.64	221.70	2085.12	887.32
	200	0.01	$\bar{Q}_{\lambda,t}^{(r)}$	1	0.9	246.16	106.39	990.62	347.18
	200	0.01	$\bar{Q}_{\lambda,t}^{(r)}$	1	0.95	43.49	8.84	237.56	57.17
	200	0.05	$P_t$			2.40	0.26	13.12	0.91
	200	0.05	$\tilde{Q}_{\lambda,t}^{(r)}$	-0.9	0.5	71.54	15.40	230.44	36.36
	200	0.05	$\tilde{Q}_{\lambda,t}^{(r)}$	-0.8	0.5	49.91	11.32	197.65	39.28
	200	0.05	$\bar{Q}_{\lambda,t}^{(r)}$	1	0.9	5.75	1.44	25.13	3.84
	200	0.05	$\bar{Q}_{\lambda,t}^{(r)}$	1	0.95	3.49	0.50	18.81	2.80
Cauchy	200	0.01	$P_t$			2.70	0.23	12.25	0.59
	200	0.01	$\tilde{Q}_{\lambda,t}^{(r)}$	-0.9	0.5	38.28	5.31	122.16	14.95
	200	0.01	$\tilde{Q}_{\lambda,t}^{(r)}$	-0.8	0.5	30.11	7.74	77.77	14.46
	200	0.01	$\bar{Q}_{\lambda,t}^{(r)}$	1	0.9	2.61	0.25	13.47	0.75
	200	0.01	$\bar{Q}_{\lambda,t}^{(r)}$	1	0.95	2.77	0.36	11.60	0.70
	200	0.05	$P_t$			1.13	0.04	5.68	0.10
	200	0.05	$\tilde{Q}_{\lambda,t}^{(r)}$	-0.9	0.5	7.00	0.92	26.34	2.92
	200	0.05	$\tilde{Q}_{\lambda,t}^{(r)}$	-0.8	0.5	4.20	0.58	12.57	0.95
	200	0.05	$\bar{Q}_{\lambda,t}^{(r)}$	1	0.9	1.13	0.04	5.70	0.11
	200	0.05	$\bar{Q}_{\lambda,t}^{(r)}$	1	0.95	1.14	0.04	5.52	0.08

Table 12: Average  $R_k$  under dynamic OOC processes for KS  $p$ -value charts  $(P_t)_t$ ,  $\left(\tilde{Q}_{\lambda,t}^{(r)}\right)_t$  and  $\left(\bar{Q}_{\lambda,t}^{(r)}\right)_t$ , using 100 simulation repetitions. This table contains results for  $n_0 = 100$ , while Appendix Tables 6 and 13 contains results for  $n_0 = 50$  and  $n_0 = 200$ , respectively.

OOC process	$n_0$	$\alpha$	Chart	$r$	$\lambda$	mean $R_1$	st. err. $R_1$	mean $R_5$	st. err. $R_5$
$N(\mu_t, 1)$	100	0.01	$P_t$			1.69	0.10	9.05	0.26
$\mu_t \sim N(0, 1/2)$	100	0.01	$\tilde{Q}_{\lambda,t}^{(r)}$	-0.9	0.5	2.72	0.22	6.84	0.23
	100	0.01	$\tilde{Q}_{\lambda,t}^{(r)}$	-0.8	0.5	2.00	0.15	6.21	0.19
	100	0.01	$\tilde{Q}_{\lambda,t}^{(r)}$	1	0.9	3.12	0.35	14.18	0.67
	100	0.01	$\bar{Q}_{\lambda,t}^{(r)}$	1	0.95	2.51	0.25	11.33	0.50
	100	0.05	$P_t$			1.67	0.10	8.04	0.22
	100	0.05	$\tilde{Q}_{\lambda,t}^{(r)}$	-0.9	0.5	1.99	0.15	6.22	0.18
	100	0.05	$\tilde{Q}_{\lambda,t}^{(r)}$	-0.8	0.5	1.98	0.17	6.09	0.18
	100	0.05	$\bar{Q}_{\lambda,t}^{(r)}$	1	0.9	2.10	0.16	9.25	0.30
	100	0.05	$\bar{Q}_{\lambda,t}^{(r)}$	1	0.95	1.70	0.13	7.86	0.22
	100	0.01	$P_t$			2.56	0.21	12.48	0.45
$\mu_t \sim N(0, 1/4)$	100	0.01	$\tilde{Q}_{\lambda,t}^{(r)}$	-0.9	0.5	3.95	0.35	9.39	0.62
	100	0.01	$\tilde{Q}_{\lambda,t}^{(r)}$	-0.8	0.5	2.81	0.23	7.67	0.37
	100	0.01	$\bar{Q}_{\lambda,t}^{(r)}$	1	0.9	5.07	0.56	23.07	1.18
	100	0.01	$\bar{Q}_{\lambda,t}^{(r)}$	1	0.95	4.61	0.46	19.82	0.98
	100	0.05	$P_t$			1.89	0.13	9.74	0.30
	100	0.05	$\tilde{Q}_{\lambda,t}^{(r)}$	-0.9	0.5	2.50	0.17	7.07	0.26
	100	0.05	$\tilde{Q}_{\lambda,t}^{(r)}$	-0.8	0.5	2.96	0.23	7.34	0.26
	100	0.05	$\bar{Q}_{\lambda,t}^{(r)}$	1	0.9	2.08	0.19	11.61	0.41
	100	0.05	$\bar{Q}_{\lambda,t}^{(r)}$	1	0.95	2.29	0.20	10.01	0.36
	100	0.01	$P_t$			2.14	0.16	10.91	0.38
$\sigma_t^2 \sim \chi_1^2$	100	0.01	$\tilde{Q}_{\lambda,t}^{(r)}$	-0.9	0.5	3.26	0.27	7.54	0.28
	100	0.01	$\tilde{Q}_{\lambda,t}^{(r)}$	-0.8	0.5	3.04	0.25	7.35	0.27
	100	0.01	$\bar{Q}_{\lambda,t}^{(r)}$	1	0.9	4.07	0.52	18.76	0.95
	100	0.01	$\bar{Q}_{\lambda,t}^{(r)}$	1	0.95	3.51	0.37	16.66	0.85
	100	0.05	$P_t$			1.94	0.14	9.32	0.30
	100	0.05	$\tilde{Q}_{\lambda,t}^{(r)}$	-0.9	0.5	3.15	0.29	7.54	0.31
	100	0.05	$\tilde{Q}_{\lambda,t}^{(r)}$	-0.8	0.5	2.59	0.17	7.14	0.24
	100	0.05	$\bar{Q}_{\lambda,t}^{(r)}$	1	0.9	2.18	0.21	10.65	0.50
	100	0.05	$\bar{Q}_{\lambda,t}^{(r)}$	1	0.95	1.91	0.14	8.94	0.30
	100	0.01	$P_t$			3.41	0.32	18.14	0.91
$\sigma_t^2 \sim \chi_2^2$	100	0.01	$\tilde{Q}_{\lambda,t}^{(r)}$	-0.9	0.5	9.01	0.95	18.93	1.41
	100	0.01	$\tilde{Q}_{\lambda,t}^{(r)}$	-0.8	0.5	7.05	0.59	16.68	1.02
	100	0.01	$\bar{Q}_{\lambda,t}^{(r)}$	1	0.9	9.14	1.20	48.17	3.24
	100	0.01	$\bar{Q}_{\lambda,t}^{(r)}$	1	0.95	5.77	0.62	31.56	1.75
	100	0.05	$P_t$			2.40	0.20	11.22	0.43
	100	0.05	$\tilde{Q}_{\lambda,t}^{(r)}$	-0.9	0.5	5.61	0.46	12.52	0.82
	100	0.05	$\tilde{Q}_{\lambda,t}^{(r)}$	-0.8	0.5	4.28	0.43	10.75	0.66
	100	0.05	$\bar{Q}_{\lambda,t}^{(r)}$	1	0.9	2.98	0.29	15.34	0.77
	100	0.05	$\bar{Q}_{\lambda,t}^{(r)}$	1	0.95	2.41	0.23	11.92	0.48

Table 13: Average  $R_k$  under dynamic OOC processes for KS  $p$ -value charts  $(P_t)_t$ ,  $\left(\tilde{Q}_{\lambda,t}^{(r)}\right)_t$  and  $\left(\bar{Q}_{\lambda,t}^{(r)}\right)_t$ , using 100 simulation repetitions. This table contains results for  $n_0 = 200$ , while Appendix Tables 6 and 12 contains results for  $n_0 = 50$  and  $n_0 = 100$ , respectively.

OOC process	$n_0$	$\alpha$	Chart	$r$	$\lambda$	mean $R_1$	st. err. $R_1$	mean $R_5$	st. err. $R_5$
$N(\mu_t, 1)$	200	0.01	$P_t$			1.49	0.07	7.69	0.20
$\mu_t \sim N(0, 1/2)$	200	0.01	$\tilde{Q}_{\lambda,t}^{(r)}$	-0.9	0.5	1.65	0.12	5.67	0.12
	200	0.01	$\tilde{Q}_{\lambda,t}^{(r)}$	-0.8	0.5	1.84	0.13	5.88	0.13
	200	0.01	$\tilde{Q}_{\lambda,t}^{(r)}$	1	0.9	1.88	0.18	9.65	0.41
	200	0.01	$\bar{Q}_{\lambda,t}^{(r)}$	1	0.95	1.71	0.14	8.65	0.29
	200	0.05	$P_t$			1.42	0.09	6.61	0.16
	200	0.05	$\tilde{Q}_{\lambda,t}^{(r)}$	-0.9	0.5	1.62	0.10	5.68	0.11
	200	0.05	$\tilde{Q}_{\lambda,t}^{(r)}$	-0.8	0.5	1.68	0.10	5.70	0.10
	200	0.05	$\bar{Q}_{\lambda,t}^{(r)}$	1	0.9	1.44	0.09	7.58	0.23
	200	0.05	$\bar{Q}_{\lambda,t}^{(r)}$	1	0.95	1.38	0.07	6.61	0.16
	200	0.01	$P_t$			1.82	0.11	9.48	0.29
$\mu_t \sim N(0, 1/4)$	200	0.01	$\tilde{Q}_{\lambda,t}^{(r)}$	-0.9	0.5	2.37	0.18	6.61	0.20
	200	0.01	$\tilde{Q}_{\lambda,t}^{(r)}$	-0.8	0.5	2.27	0.17	6.61	0.19
	200	0.01	$\bar{Q}_{\lambda,t}^{(r)}$	1	0.9	2.99	0.31	12.85	0.62
	200	0.01	$\bar{Q}_{\lambda,t}^{(r)}$	1	0.95	2.49	0.22	12.28	0.53
	200	0.05	$P_t$			1.40	0.08	7.94	0.23
	200	0.05	$\tilde{Q}_{\lambda,t}^{(r)}$	-0.9	0.5	2.15	0.17	6.29	0.18
	200	0.05	$\tilde{Q}_{\lambda,t}^{(r)}$	-0.8	0.5	1.92	0.13	6.05	0.15
	200	0.05	$\bar{Q}_{\lambda,t}^{(r)}$	1	0.9	1.85	0.15	8.84	0.27
	200	0.05	$\bar{Q}_{\lambda,t}^{(r)}$	1	0.95	1.52	0.10	7.92	0.22
	200	0.01	$P_t$			1.68	0.10	8.81	0.28
$\sigma_t^2 \sim \chi_1^2$	200	0.01	$\tilde{Q}_{\lambda,t}^{(r)}$	-0.9	0.5	2.00	0.16	6.11	0.17
	200	0.01	$\tilde{Q}_{\lambda,t}^{(r)}$	-0.8	0.5	2.13	0.17	6.40	0.22
	200	0.01	$\bar{Q}_{\lambda,t}^{(r)}$	1	0.9	2.54	0.23	11.91	0.56
	200	0.01	$\bar{Q}_{\lambda,t}^{(r)}$	1	0.95	2.06	0.19	9.76	0.38
	200	0.05	$P_t$			1.44	0.07	7.35	0.18
	200	0.05	$\tilde{Q}_{\lambda,t}^{(r)}$	-0.9	0.5	1.80	0.12	5.93	0.14
	200	0.05	$\tilde{Q}_{\lambda,t}^{(r)}$	-0.8	0.5	1.75	0.13	5.84	0.14
	200	0.05	$\bar{Q}_{\lambda,t}^{(r)}$	1	0.9	1.54	0.11	8.04	0.27
	200	0.05	$\bar{Q}_{\lambda,t}^{(r)}$	1	0.95	1.56	0.08	7.57	0.20
	200	0.01	$P_t$			2.22	0.16	10.53	0.31
$\sigma_t^2 \sim \chi_2^2$	200	0.01	$\tilde{Q}_{\lambda,t}^{(r)}$	-0.9	0.5	3.36	0.28	8.59	0.40
	200	0.01	$\tilde{Q}_{\lambda,t}^{(r)}$	-0.8	0.5	3.65	0.32	8.52	0.42
	200	0.01	$\bar{Q}_{\lambda,t}^{(r)}$	1	0.9	3.57	0.32	16.76	1.04
	200	0.01	$\bar{Q}_{\lambda,t}^{(r)}$	1	0.95	3.05	0.35	16.25	0.86
	200	0.05	$P_t$			1.59	0.10	8.24	0.26
	200	0.05	$\tilde{Q}_{\lambda,t}^{(r)}$	-0.9	0.5	2.63	0.22	7.11	0.26
	200	0.05	$\tilde{Q}_{\lambda,t}^{(r)}$	-0.8	0.5	2.53	0.19	6.86	0.20
	200	0.05	$\bar{Q}_{\lambda,t}^{(r)}$	1	0.9	2.04	0.18	10.08	0.45
	200	0.05	$\bar{Q}_{\lambda,t}^{(r)}$	1	0.95	1.82	0.13	8.51	0.31

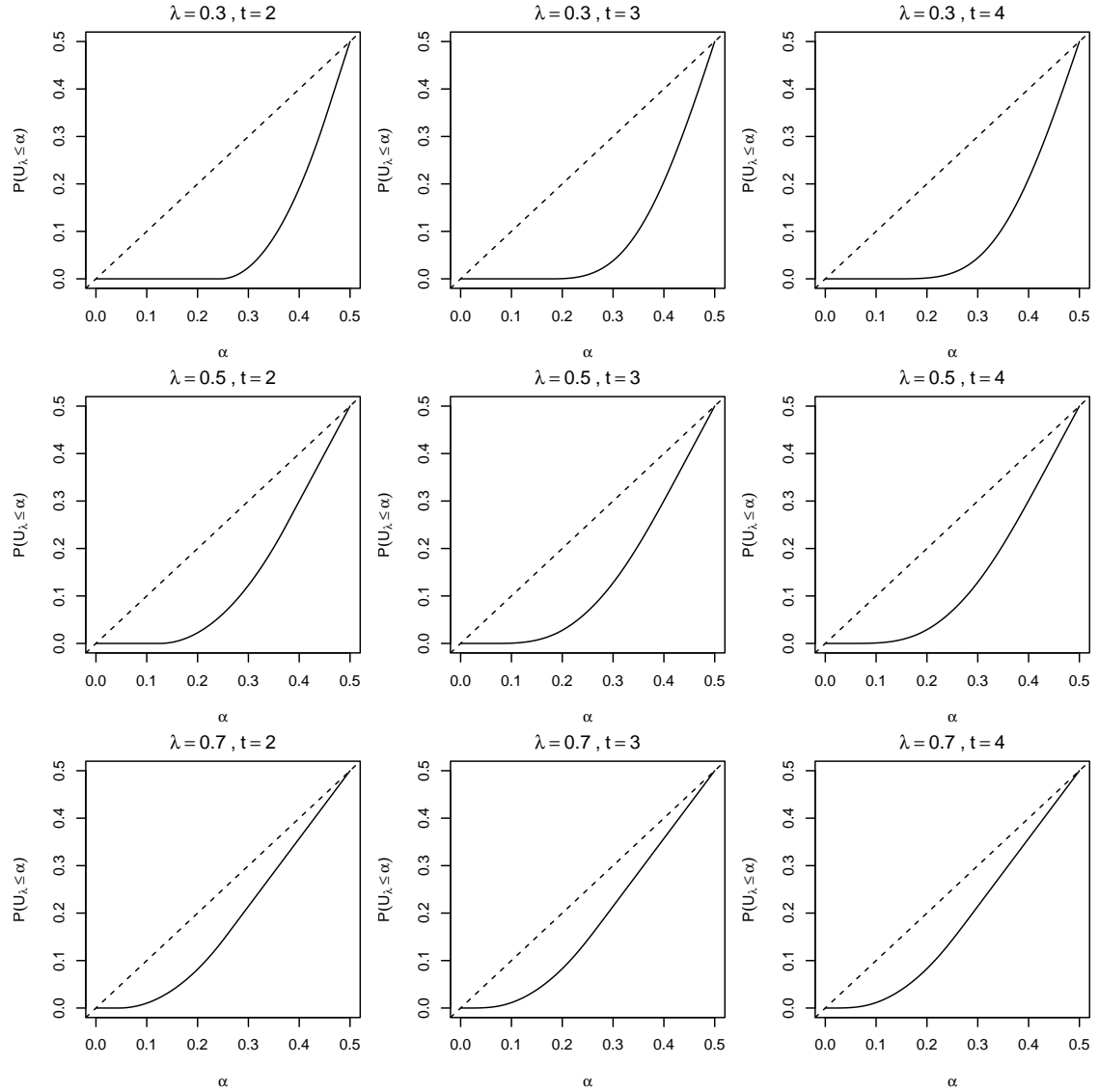


Figure 2: Plots of CDFs of the random variables  $\tilde{U}_{\lambda,t}$  with initialisation  $u_0 = 1/2$ , i.e.,  $F(\alpha) = P_0(\tilde{U}_{\lambda,t} \leq \alpha)$ , for  $\lambda \in \{0.3, 0.5, 0.7\}$  and  $t \in \{2, 3, 4\}$  (solid line) along with the CDF of  $U \sim \text{Unif}[0, 1]$  (dashed line) for  $\alpha \leq 1/2$ .

Table 14: Average run lengths  $R$ , numbers of detected OOC directions at time of alarm  $\#\text{OOC}$ , and numbers of single time point family wise errors (at time  $t = 1$ ) for  $d = 3$  variable Cauchy model with  $n_0 = 20$  tested using the procedure from Section 3.1 with Mann–Whitney  $U$ -tests. Average run lengths and number of true positives are reported via 100 simulation replications, while single time point family wise errors are obtained from 10000 simulations.

$\delta$	$\rho$	$\alpha$	Mean $R$	Mean $\#\text{OOC}$	Mean FWEs
0.5	0	0.01	397	0.78	0.0031
0.5	0	0.05	90.17	0.73	0.0184
0.5	0.5	0.01	1762.03	0.83	0.0041
0.5	0.5	0.05	37.99	0.9	0.0193
0.5	0.9	0.01	2963.58	0.94	0.0051
0.5	0.9	0.05	82.84	0.99	0.0295
1	0	0.01	68.74	1.01	0.0038
1	0	0.05	8.07	1.05	0.0211
1	0.5	0.01	1052.82	0.97	0.0045
1	0.5	0.05	4.77	1.03	0.0217
1	0.9	0.01	44.74	1	0.0054
1	0.9	0.05	6.05	1.01	0.023

Table 15: Average run lengths  $R$ , numbers of detected OOC directions at time of alarm  $\#\text{OOC}$ , and numbers of single time point family wise errors (at time  $t = 1$ ) for  $d = 3$  variable Cauchy model with  $n_0 = 100$  tested using the procedure from Section 3.1 with Mann–Whitney  $U$ -tests. Average run lengths and number of true positives are reported via 100 simulation replications, while single time point family wise errors are obtained from 10000 simulations.

$\delta$	$\rho$	$\alpha$	Mean $R$	Mean $\#\text{OOC}$	Mean FWEs
0.5	0	0.01	17.45	1.06	0.0042
0.5	0	0.05	2.65	1.12	0.0259
0.5	0.5	0.01	9.9	1.01	0.0055
0.5	0.5	0.05	2.69	1.12	0.0238
0.5	0.9	0.01	6.58	1	0.0052
0.5	0.9	0.05	2.23	1.04	0.0298
1	0	0.01	1.1	1.67	0.0078
1	0	0.05	1	1.81	0.0468
1	0.5	0.01	1.03	1.68	0.0073
1	0.5	0.05	1	1.78	0.0427
1	0.9	0.01	1	1.64	0.0059
1	0.9	0.05	1	1.84	0.0326